Geochemistry Geophysics Geosystems G3
AN ELECTRONIC JOURNAL OF THE EARTH SCIENCES
Published by AGU and the Geochemical Society

Article
Volume 5, Number 3
6 March 2004
Q03G13, doi:10.1029/2002GC000434
ISSN: 1525-2027

Composition of basaltic lavas sampled by phase-2 of the Hawaii Scientific Drilling Project: Geochemical stratigraphy and magma types

J. M. Rhodes and M. J. Vollinger
Department of Geosciences, University of Massachusetts, Amherst, Massachusetts 01003, USA (jmrhodes@geo.umass.edu)

[1] This paper presents major and trace element compositions of lavas from the entire 3098 m stratigraphic section sampled by phase-2 of the Hawaii Scientific Drilling Project. The upper 245 m are lavas from Mauna Loa volcano, and the lower 2853 m are lavas and volcanoclastic rocks from Mauna Kea volcano. These intervals are inferred to represent about 100 ka and 400 ka respectively of the eruptive history of the two volcanoes. The Mauna Loa tholeiites tend to be higher in SiO_2 and lower in total iron, TiO_2, alkalis, and incompatible elements at a given MgO content than Mauna Kea lavas. The transition from Mauna Loa to Mauna Kea lavas is all the more pronounced because the Mauna Loa tholeiites overlie a thin sequence of postshield Mauna Kea alkalic to transitional tholeiitic lavas. The Mauna Loa tholeiites display well-developed coherent trends with MgO that are indistinguishable in most respects from modern lavas. With depth, however, there is a slight decline in incompatible element abundances, and small shifts to depleted isotopic ratios. These characteristics suggest small changes in melt production and source components over time, superimposed on shallow melt segregation. The Mauna Kea section is subdivided into a thin, upper 107 m sequence of postshield tholeiites, transitional tholeiites and alkali basalts of the Hamakua volcanics, overlying four tholeiitic magma types that are intercalated throughout the rest of the core. These four magma types are recognized on the basis of MgO-normalized SiO_2 and Zr/Nb values. Type-1 lavas (high SiO_2 and Zr/Nb) are ubiquitous below the postshield lavas and are the dominant magma type on Mauna Kea. They are inter-layered with the other three lava types. Type-2 lavas (low SiO_2 but high Zr/Nb) are found only in the upper core, and especially above 850 m. Type-3 lavas (low SiO_2 and Zr/Nb) are very similar to tholeiites from Loihi volcano and are present only below 1974 m. There are only 3 discrete samples of type-4 lavas (high SiO_2 and low Zr/Nb), which are present in the upper and lower core. The differences between these magma types are inferred to reflect changes in melt production, depth of melt segregation, and differences in plume source components over about 400 ka of Mauna Kea's eruptive history. At the start of this record, eruption rates were high, and two distinct tholeiitic magmas (type-1 and 3) were erupting concurrently. These two magmas require two distinct source components, one similar to that of modern Loihi tholeiites and the other close to that of Kilauea magmas. Subsequently, the Loihi-like source of the type-3 magmas was exhausted, and these lavas are absent from the remainder of the core. For the next 200 ka or so, the eruptive sequence consists of inter-layered type-1 and -2 lavas that are derived from a common Mauna Kea source, the major difference between the two being the depth at which the melts segregated from the source. At around 440 ka (corresponding with the transition in the core from submarine to subaerial lavas) eruption rates began to decline and low-MgO lavas are suddenly much more abundant in the record. Continuing gradual decline in melting and eruption rates was accompanied by a decline in normalized SiO_2 content of the type-1 magmas, and the eventual onset of postshield magmatism.

Components: 30,168 words, 16 figures, 4 tables.

Keywords: Basalt Hawaii; plume.

Index Terms: 3640 Mineralogy and Petrology: Igneous petrology; 3655 Mineralogy and Petrology: Major element composition; 1065 Geochemistry: Trace elements (3670).

Received 29 August 2002; **Revised** 4 November 2003; **Accepted** 13 November 2003; **Published** 6 March 2004.

Rhodes, J. M., and M. J. Vollinger (2004), Composition of basaltic lavas sampled by phase-2 of the Hawaii Scientific Drilling Project: Geochemical stratigraphy and magma types, *Geochem. Geophys. Geosyst.*, *5*, Q03G13, doi:10.1029/2002GC000434.

Theme: Hawaii Scientific Drilling Project **Guest Editors:** Don DePaolo, Ed Stolper, and Don Thomas

1. Introduction

[2] Recent concepts concerning the Hawaiian plume suggest that it is concentrically zoned, both thermally and compositionally [e.g., *Griffith and Cambell*, 1990; *Watson and Mackenzie*, 1991; *Frey and Rhodes*, 1993; *Hauri et al.*, 1994; *Kurz et al.*, 1995; *Rhodes and Hart*, 1995; *Lassiter et al.*, 1996; *Ribe and Christenson*, 1999]. According to these models, as the Pacific plate moves over the stationary plume at a rate of about 9–10 cm/year, a volcano is produced from magma generated in the melting zone of the rising plume. At the cooler margins of the melt zone, melt production is low, leading to the initiation of volcanism on the ocean floor, with low eruption rates and the eruption of alkalic and transitional tholeiitic basalts during the pre-shield stage of volcanism. This is followed by the voluminous shield-building stage as the volcano tracks over a zone of maximum melt generation within the plume. This stage is characterized by very high eruption rates of tholeiites, olivine tholeiites and picrites, and is responsible for forming 95–98 percent of the volume of the volcano [*Macdonald*, 1963]. Inexorably, the volcano moves away from the axis of the melt zone, magma supplies and eruption rates dwindle, leading to the postshield stage, which is characterized by a thin veneer of intercalated alkalic basalts, transitional tholeiites and tholeiites. Superimposed on this radial thermal structure is compositional zoning, consisting of a central plume core surrounded by concentric zones of entrained lower mantle and asthenosphere. Inter-volcano compositional variations [e.g., *Frey and Rhodes*, 1993] are commonly interpreted in terms of this proposed concentric zoning. It should be stressed, however, that the impetus for these models comes largely from fluid dynamics [e.g., *Hauri et al.*, 1994; *Ribe and Christenson*, 1999]. The most compelling volcanological or geochemical evidence to date is that the model satisfactorily accounts for the growth and evolution of Hawaiian volcanoes, [*Stearns*, 1946; *Clague and Dalrymple*, 1987; *Moore and Clague*, 1992], and for the presence of Loihi, a submarine volcano on the so-called Loa trend [*Tatsumoto*, 1978], that has compositional characteristics similar to those of Kea trend volcanoes.

[3] The Hawaii Scientific Drilling Project (HSDP) drill hole was designed to systematically sample a stratigraphic sequence of lavas from Mauna Kea volcano in order to test and modify these concepts. The project is based on the assumption that changes in lava compositions and eruption rates will reflect changes in source components and melt production as the volcano transits the zoned mantle plume. To date, core of basaltic lavas has been recovered to a depth of 3098 m [*Hawaii Scientific Drilling Project-2*, 2000]. For logistical reasons, the drill hole sampled 245 m of subaerial Mauna Loa lavas before penetrating into subaerial and submarine Mauna Kea lavas. Subaerial Mauna Kea lavas extend to a depth of 1080 m, and are underlain by a further 2018 m of submarine pillow lavas, hyaloclastites and massive and intrusive units [*Seaman et al.*, 2000]. Dating of these lavas [*Sharp et al.*, 1996; W. D. Sharp, P. R. Renne, and T. A. Becker, The $^{40}Ar/^{39}Ar$ and K/Ar dating of lavas, hyaloclastites and intrusions from the HSDP core hole, manuscript submitted to *Geochemistry*

Geophysics Geosystems, 2003, hereinafter referred to as Sharp et al., submitted manuscript, 2003], together with lava accumulation rate models for Mauna Kea [*DePaolo and Stolper*, 1996; D. J. DePaolo, E. M. Stolper, W. Sharp, and P. Renne, Lifetimes, lava accumulation, and geochemical patterns of Hawaiian volcanoes: Inferences from HSDP data and plume models, manuscript in preparation, 2003] indicate that about 400 ka of the eruptive record may have been sampled, from the oldest submarine lavas of around 550 ka to the youngest subaerial postshield lavas at about 150–180 ka.

[4] This paper presents major and trace element data for lavas sampled throughout the entire 3098 m stratigraphic section. The principle goals of the study are (1) to identify the change from Mauna Loa to Mauna Kea lavas, and to examine the extent to which flows from these two contemporaneously erupting volcanoes are inter-layered; (2) to evaluate compositional changes with depth (increasing age), in particular, the presence and distribution of different magma types, and whether there are systematic changes in magma composition over time; (3) to use this information to improve understanding of the magmatic evolution of both Mauna Kea and Mauna Loa volcanoes as they transit the Hawaiian plume.

2. Sampling and Analytical Methods

[5] To fully characterize the composition of the core, our aim was to analyze every flow unit in the subaerial section of the core, and to maximize sampling frequency in the submarine section. In fact, a small number of flows in the subaerial section were unsuitable for analysis, and sampling of pillow lavas, hyaloclastites, intrusive and massive units in the submarine section was dictated by the availability of relatively fresh material of a suitable size. Therefore in addition to the 119 reference samples selected to characterize the core [*Seaman et al.*, 2000] we have sampled and analyzed a further 170 samples, for a total of 289 analyzed samples. This sampling scheme has led to sampling densities of about every 5 m for Mauna Loa flows, 6 m for subaerial Mauna Kea flows, and 19 m for the submarine Mauna Kea section.

[6] The sample crushing and washing protocols were identical to those described by *Rhodes* [1996], as were the X-ray fluorescence (XRF) analytical methods for major and trace elements, the major difference being that the trace elements (Rb, Sr, Ba, Ce, Nb, Zr, Y, Pb, Zn, Ga, Ni, Cr, V) were measured on a Philips PW2400 sequential spectrometer. This instrument uses a Rh tube, so that mass absorption coefficients were estimated from the intensity of the Rh Compton peak. Estimates of the precision and accuracy of these data are given by *Rhodes* [1988, 1996] and from Table 1, which contains a single analysis of the U.S.G.S. standard BHVO-1 and six replicate analyses of KIL-1919, a sample of the 1919 Kilauea summit flow, from which the U.S.G.S. standard BHVO-1 was obtained. Note that this flow is slightly heterogeneous [*Garcia et al.*, 2004] and there are small differences in composition between BHVO-1 and KIL-1919.

[7] In addition to the customary major and trace elements determined by XRF, we also measured loss on ignition (LOI) and ferrous iron content in order to provide additional information on alteration of the samples (M. J. Vollinger and J. M. Rhodes, Chemical alteration in basalts sampled by phase-2 of the Hawaii Scientific Drilling Project, manuscript in preparation, 2003). Loss on ignition was measured gravimetrically by weighing 2 to 5 g of sample before and after heating at 1020°C in a muffle furnace. Although LOI is widely used as a measure of volatile content and alteration, there are serious problems with this measurement because, in addition to the sample losing water and other volatiles on heating, it may also gain weight through oxidation of ferrous iron. To minimize weight gain through oxidation, the heating time was limited to 10 minutes. Nonetheless, many of the fresher samples gained weight resulting in negative LOI values. Ferrous iron measurements were made in duplicate on separate 150–200 mg aliquants of powder using a modification of the Wilson cold acid digestion titrimetric technique [*Maxwell*, 1968]. The resulting FeO data were then used,

Table 1. Data for the HSDP Standard Kil-1919 and the USGS Standard BHVO-1

	BHVO-1	Kil-1919	Kil-1919	Kil-1919	Kil-1919	Kil-1919	Kil-1919	Kil-1919	Kil-1919
		(1)	(2)	(3)	(4)	(5)	(6)	Avg.	Std. Dev.
SiO_2	49.58	49.99	49.97	49.95	50.06	50.01	50.02	50.00	0.04
TiO_2	2.740	2.757	2.767	2.766	2.776	2.765	2.767	2.766	0.006
Al_2O_3	13.61	13.70	13.73	13.73	13.79	13.72	13.74	13.74	0.03
Fe_2O_3	12.17	12.08	12.08	12.11	12.09	12.07	12.10	12.09	0.01
MnO	0.170	0.177	0.176	0.177	0.176	0.176	0.178	0.180	0.001
MgO	7.09	6.89	6.88	6.88	6.88	6.88	6.90	6.88	0.01
CaO	11.35	11.41	11.42	11.41	11.43	11.41	11.41	11.42	0.01
Na_2O	2.40	1.84	1.81	1.83	1.68	1.79	1.74	1.78	0.06
K_2O	0.522	0.522	0.525	0.540	0.541	0.526	0.525	0.530	0.008
P_2O_5	0.272	0.272	0.274	0.275	0.275	0.275	0.273	0.274	0.001
Total	99.90	99.64	99.63	99.67	99.70	99.62	99.65	99.65	
Nb	18.7	18.6	18.2	18.3	18.4	18.3	18.4	18.4	0.11
Zr	181.0	178.0	176.8	176.5	176.7	175.9	176.4	176.7	0.63
Y	25.5	24.9	24.7	24.5	24.7	24.7	24.7	24.7	0.10
Sr	383.1	397.5	394.8	394.8	394.6	393.4	392.7	394.6	1.50
Rb	9.2	9.0	9.1	9.1	9.0	8.9	9.0	9.0	0.08
Th	1.6	0.8	1.2	0.6	1.1	1.4	0.7	1.0	0.30
Pb	1.4	1.2	1.5	1.8	1.6	1.2	1.6	1.5	0.24
Ga	20.9	21.1	21.1	21.2	21.0	21.2	20.7	21.0	0.16
Zn	113.3	107.5	107.1	106.7	106.5	106.3	107.8	107.0	0.54
Ni	114.3	101.6	100.5	101.1	100.9	100.1	101.2	100.9	0.50
Cr	296.7	265.7	264.8	269.0	268.4	266.9	263.5	266.4	1.94
V	294.7	284.3	284.9	283.4	282.2	284.2	284.1	283.8	0.87
Ce	40.8	40.1	40.5	38.3	38.2	39.1	38.3	39.1	0.91
Ba	127.5	124.4	123.7	125.0	125.5	123.6	122.1	124.0	1.12
La	17.7	16.5	12.9	12.8	14.0	20.2	14.2	15.1	2.59

in conjunction with the XRF total iron as Fe_2O_3 data, to calculate ferric/ferrous ratios.

3. Discriminating Between Mauna Loa and Mauna Kea Lavas

[8] Lavas from adjacent Hawaiian volcanoes are often distinctly different in composition. These differences apply to the major elements [e.g., *Powers*, 1955; *Wright*, 1971; *Rhodes et al.*, 1989; *Frey and Rhodes*, 1993; *Hauri*, 1996], and to trace elements [e.g., *Budahn and Schmitt*, 1985; *Rhodes et al.*, 1989; *Frey and Rhodes*, 1993], and have been widely documented for isotopic ratios [e.g., *Tatsumoto*, 1978; *Staudigal et al.*, 1984; *West et al.*, 1987; *Frey and Rhodes*, 1993; *Lassiter and Hauri*, 1998]. Several recent studies [e.g., *Lipman et al.*, 1990; *Chen et al.*, 1996; *Quane et al.*, 2000] suggest that these differences may persist for over 100 ka or more.

[9] The use of chemical discriminants to distinguish between Mauna Loa and Mauna Kea lavas was addressed by *Rhodes* [1996] during the pilot hole drilling for the current project. At a given MgO content, Mauna Kea lavas are systematically lower in SiO_2 and higher in total alkalis, Fe_2O_3, TiO_2 and incompatible elements, than Mauna Loa lavas. The most effective discriminants, however, are TiO_2/Al_2O_3 among the major elements, and trace element ratios involving Nb (e.g., Zr/Nb, Sr/Nb and Nb/Y). The latter is because Nb abundances and incompatible element ratios involving Nb correlate strongly with isotopic ratios [e.g., *Frey and Rhodes*, 1993; *Rhodes and Hart*, 1995; *Chen et al.*, 1996] and therefore reflect differences in the proportions of source components in the Hawaiian plume more strongly than the effects of melting.

[10] Flows above 245 m (flow units 1–41) have high Zr/Nb and low TiO_2/Al_2O_3 (characteristics typical of Mauna Loa lavas), whereas those below 245 m (flow units 42–345) have lower Zr/Nb and higher TiO_2/Al_2O_3 (characteristics typical of Mauna Kea lavas). Nb/Y, Ba/Nb and Sr/Nb ratios also confirm that the transition from Mauna Loa to

Mauna Kea lavas occurs at a depth of 245 m in the core. The location of the actual transition is made even clearer (Figure 1) because the uppermost of the Mauna Kea flows are transitional tholeiites and alkalic basalts of the Hamakua Volcanics [*Frey et al.*, 1990; *Wolfe et al.*, 1997], with TiO_2/Al_2O_3, Nb/Y, Ba/Y, Zr/Y, and many other trace element ratios that are quite distinct from those of Mauna Loa. Surprisingly, there is no evidence for inter-fingering of flows from the two volcanoes, despite the fact that both volcanoes were erupting between 100 to 200 ka ago [*Sharp et al.*, 1996]. Note that in Figure 1 the Mauna Kea tholeiites below the postshield Hamakua volcanics, have been subdivided into four magma-types as detailed in the following section.

4. Geochemical Stratigraphy

[11] Major and trace element data for the 289 samples analyzed in this study are presented in Tables 2 and 3. They are organized according to stratigraphic depth within the drill core. Sample numbers for the reference samples are shown in regular type, whereas sample numbers for samples from additional flow units, or additional samples from the same reference flow units are shown in italic type. Wherever possible, samples have been distinguished as flows, pillow lavas, hyaloclastites and massive or intrusive units. We have adopted the project's convention of designating a sample by its run number and the uppermost core interval from which the sample was taken (e.g., SR36-2.1 indicates a sample from 2.1 feet, measured from the start of run 36). Additionally, in Tables 2 and 3, we have included information on the sample interval from which the sample that was actually analyzed was taken. This is because in some cases, the portion analyzed comes from a significantly different interval from that used to identify the reference sample.

4.1. Mauna Loa Lavas

[12] The uppermost 245 m of the drill hole sampled 41 flow units from Mauna Loa volcano. All are strongly tholeiitic (Figures 2 and 3), with a wide range in MgO content from 6.5–29.7% (Figure 4). Within this range, however, there is a bi-modal distribution: a dense compositional group of lavas with MgO contents between 7–10 wt.%, and a more varied group of lavas with more than 13 wt.% MgO (Figures 4–6). According to *Le Bas* [2000], basalts with more than 12% MgO are, strictly speaking, picrites, making the two groups olivine tholeiites and picrites respectively. The MgO content of the lavas and are not correlated with depth (Figure 4); picritic lavas are interlayered, throughout the Mauna Loa section of the core, with the lower MgO lavas. There is, however, a distinct increase in the lowest MgO content of the lower-MgO lava group with increasing depth (Figure 4). The two compositional groups and the wide spread in MgO content, contrasts with our earlier results from the HSDP pilot hole project [*Rhodes*, 1996]. In that study, only a few low-MgO lavas were recorded, and most of the samples contained more than 9 wt.% MgO. The present range in MgO values, and the presence of lower MgO lavas, is much closer to the range (6.3–22.2% MgO) typically found in historical (1843–1984) and young (<36 ka) prehistoric Mauna Loa lavas [*Rhodes*, 1988, 1995; *Rhodes and Hart*, 1995; Rhodes, unpublished data]. Nonetheless, the proportion of picrites is still greater among the HSDP samples than among historical and young prehistoric lavas. We attribute these different results to a difference in sampling strategies. In the pilot hole project, sampling preference was given to massive flow units, whereas in this study we have attempted to sample and analyze every flow unit, providing a fuller, more representative, sampling of the stratigraphic record.

[13] The strongly coherent linear correlations between MgO and other oxides and trace elements (Figures 5–7) are typical of Mauna Loa lavas. Very few lavas show evidence of iron-enrichment or fractionation beyond olivine-control. For most major and compatible trace elements, these trends are remarkably similar to the trends observed in historical Mauna Loa lavas. Incompatible trace elements, however, do tend to be slightly lower in abundance, at a given MgO content, than in historical lavas, but not significantly below values found in the more depleted of the historical lavas erupted around 1880–1887 [*Rhodes and Hart*,

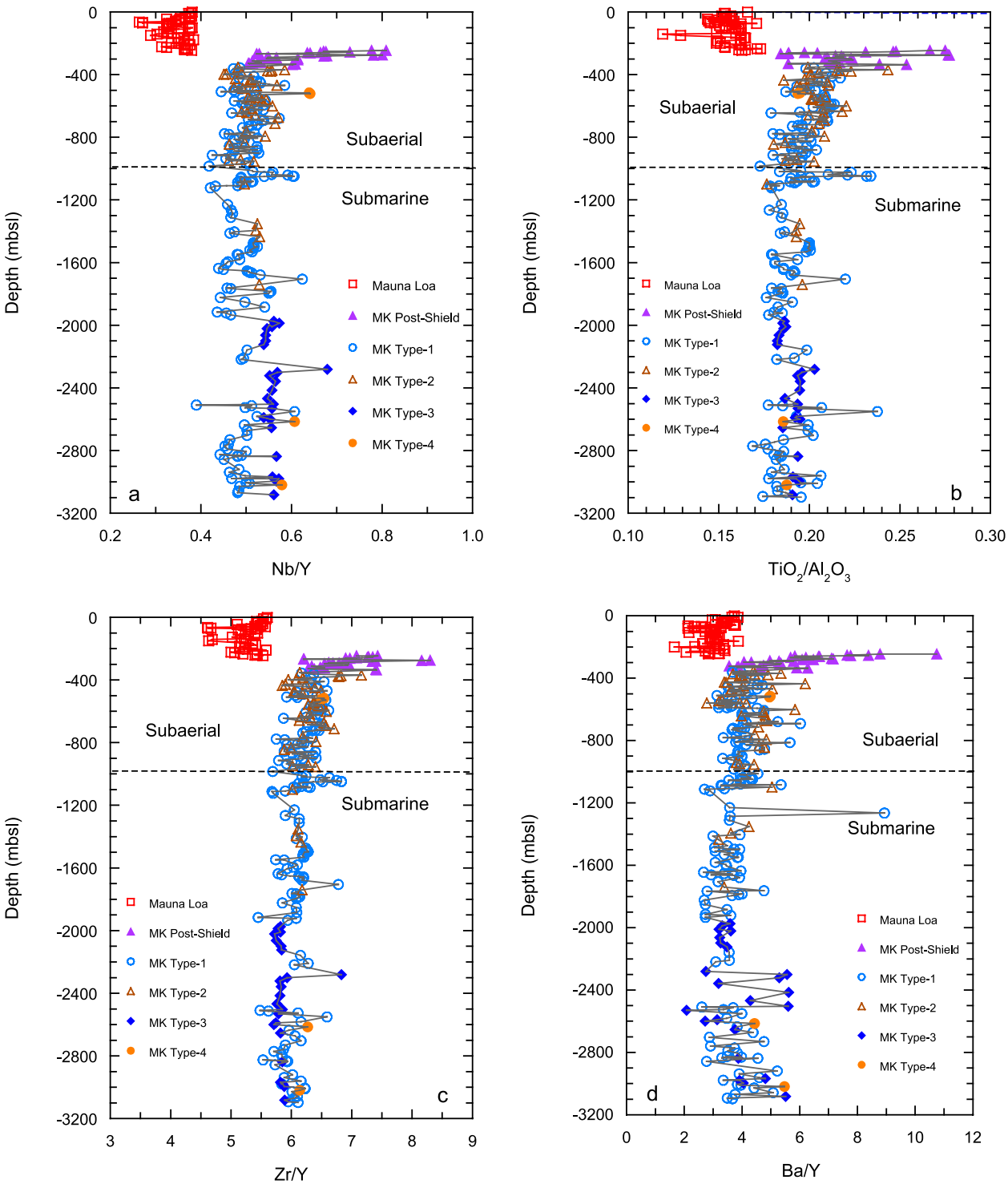

Figure 1. Variations of (a) Nb/Y, (b) TiO_2/Al_2O_3, (c) Zr/Y, and (d) Ba/Y with stratigraphic depth below sea level (mbsl) in samples from HSDP-2. The change from Mauna Loa lavas to Mauna Kea lavas at a depth of 245 m is clearly evident. The Mauna Kea lavas have been subdivided into postshield lavas and four underlying tholeiitic lava types. These distinctions are explained in the text.

Table 2 (Representative Sample). Major Element Analyses of Lavas Sampled by the HSDP-2 Core[a] (The full Table 2 is available in the HTML version of this article at http://www.g-cubed.org)

Sample ID	Run and Core Interval	Unit #	Depth (mbsl)	Rock Type	Chem. Type	SiO_2, %	TiO_2, %	Al_2O_3, %	Fe_2O_3*, %	MnO, %	MgO, %	CaO, %	Na_2O, %	K_2O, %	P_2O_5, %	Total, %
SR0002-1.00	R2-1.0-2.0	1	−1.5	FL	ML	51.81	2.25	13.57	12.51	0.18	6.51	10.28	2.26	0.45	0.28	100.10
SR0008-0.30	R8-0.3-0.8	2	−8.8	FL	ML	51.31	2.09	13.65	11.91	0.17	7.48	10.51	2.17	0.40	0.25	99.93
SR0008-2.70	R8-3.4-4.2	2	−9.5	FL	ML	51.32	2.08	13.56	11.93	0.17	7.64	10.42	2.08	0.41	0.25	99.85
SR0018-0.10	R18-0.1-0.8	4	−25.7	FL	ML	49.53	1.72	11.00	12.29	0.17	14.50	8.54	1.61	0.30	0.19	99.85
SR0019-1.30	R19-1.3-1.9	5	−27.4	FL	ML	49.80	1.73	11.42	12.11	0.17	13.59	8.90	1.48	0.30	0.19	99.68
SR0022-4.30	R22-4.3-4.9	6	−33.1	FL	ML	49.66	1.68	11.06	12.12	0.17	14.56	8.64	1.71	0.30	0.19	100.08
SR0023-2.90	R23-2.90-3.60	6	−34.0	FL	ML	49.79	1.78	11.41	12.25	0.17	13.18	8.89	1.76	0.32	0.20	99.74
SR0028-2.20	R28-2.2-2.8	7	−41.6	FL	ML	46.92	1.24	8.02	12.28	0.17	22.58	6.72	1.17	0.24	0.15	99.49
SR0031-0.50	R31-1.25-2.0	7	−45.5	FL	ML	45.01	0.86	5.95	12.59	0.17	28.68	5.29	0.75	0.13	0.09	99.53
SR0034-3.60	R34-3.6-4.5	8	−50.8	FL	ML	48.87	1.48	9.91	11.70	0.17	17.02	8.51	1.72	0.28	0.18	99.85
SR0036-1.22	R36-2.1-2.9	8	−53.4	FL	ML	46.37	1.16	7.35	12.52	0.18	24.24	6.41	1.13	0.21	0.14	99.70
SR0040-0.00	R40-0.0-0.9	9	−59.2	FL	ML	45.23	0.92	6.39	12.47	0.17	27.46	5.74	0.92	0.14	0.11	99.56
SR0040-1.07	R40-2.05-3.0	9	−59.5	FL	ML	45.54	1.00	6.31	12.58	0.17	27.28	5.54	0.97	0.20	0.12	99.70
SR0043-1.20	R43-1.2-1.8	11	−64.1	FL	ML	50.69	2.03	13.73	12.07	0.18	7.91	10.90	2.01	0.25	0.21	99.97
SR0046-1.15	R46-1.5-2.0	11	−68.8	FL	ML	50.58	2.04	13.79	12.04	0.18	7.72	10.82	2.22	0.26	0.22	99.86
SR0046-0.30	R46-0.3-0.8	12	−68.4	FL	ML	50.77	2.02	13.89	11.91	0.18	7.69	10.84	2.02	0.26	0.21	99.79
SR0049.03	R49-0.3-0.8	13	−72.9	FL	ML	51.49	2.24	13.12	12.56	0.18	7.76	10.37	1.40	0.32	0.23	99.67
SR0050-3.30	R50-3.3-3.8	14	−75.4	FL	ML	50.66	2.17	13.39	12.58	0.18	8.53	10.27	1.16	0.25	0.22	99.41
SR0054-0.1	R54-0.1-0.8	15	−79.9	FL	ML	50.14	2.11	13.40	12.58	0.18	8.95	10.33	1.86	0.22	0.21	99.98
SR0057-3.00	R57-3.75-4.5	15	−85.9	FL	ML	50.51	1.96	13.01	12.31	0.18	9.80	10.11	1.84	0.21	0.19	100.12
SR0059-4.10	R59-4.1-4.7	16	−89.4	FL	ML	51.15	2.03	13.22	12.18	0.18	8.76	10.32	2.00	0.28	0.20	100.30
SR0061-0.00	R61-0.65-1.30	16	−91.2	FL	ML	50.29	2.06	12.69	12.78	0.18	9.96	9.82	1.82	0.23	0.20	100.03
SR0066-4.10	R66-4.1-4.6	17	−100.1	FL	ML	44.23	1.01	6.31	13.06	0.18	29.71	4.62	0.75	0.07	0.10	100.03
SR0066-0.00	R67-0.40-1.30	18	−100.3	FL	ML	44.35	1.02	6.46	12.84	0.17	28.99	4.92	0.81	0.08	0.10	99.74
SR0070-4.50	R70-4.5-4.8	18	−106.3	FL	ML	47.49	1.59	9.89	12.46	0.17	18.38	7.95	1.43	0.19	0.16	99.72
SR0073-0.00	R73-0.0-0.7	19	−109.5	FL	ML	50.92	2.04	12.65	12.59	0.18	9.51	9.87	1.94	0.31	0.20	100.19
SR0080-0.35	R80-1.22-2.0	19	−125.5	FL	ML	51.10	2.02	13.60	12.14	0.18	8.08	10.55	1.96	0.26	0.19	100.08
SR0083-7.10	R83-7.1-7.6	20	−136.8	FL	ML	50.67	2.16	13.58	12.34	0.18	8.10	10.54	2.06	0.22	0.21	100.06
SR0083-7.85	R83-8.50-9.20	20	−137.1	FL	ML	49.91	2.12	13.03	12.60	0.18	9.18	10.26	1.97	0.19	0.20	99.63
SR0085-1.10	R85-1.1-1.6	22	−141.1	FL	ML	49.98	1.90	15.93	11.30	0.16	7.82	10.65	2.12	0.12	0.17	100.16
SR0089-1.15	R89-1.15-1.85	22	−149.9	FL	ML	49.91	1.88	14.58	11.61	0.17	8.88	10.77	1.98	0.13	0.17	100.08
SR0093-6.55	R93-6.55-7.4	26	−163.3	FL	ML	49.85	2.23	13.60	12.95	0.19	8.78	10.21	1.74	0.11	0.19	99.84
SR0094-8.10	R94-8.1-8.6	26	−167.0	FL	ML	50.66	2.23	13.51	12.86	0.18	8.67	9.95	1.86	0.20	0.18	100.31
SR0098-2.00	R98-2.78-3.50	28	−177.8	FL	ML	47.22	1.46	9.02	12.33	0.17	20.77	7.20	1.31	0.23	0.14	99.84
SR0098-5.10	R98-5.1-5.7	28	−178.7	FL	ML	47.57	1.54	9.48	12.48	0.17	19.29	7.57	1.35	0.24	0.15	99.82

[a] Rock types: FL, subaerial flows; HY, hyaloclasties; MA, massive units; PI, pillows; IN, intrusives. Chem. Type, Chemical Type, i.e., ML is Mauna Loa, PS is Mauna Kea Post-Shield, MK-1 is Mauna Kea Type-1, MK-2 is Mauna Kea Type-2, MK-3 is Mauna Kea Type-3 and MK-4 is Mauna Kea Type-4. Fe_2O_3* is total iron expressed as Fe_2O_3. Mg# is Mg/(Mg + Fe) after adjusting Fe_3+/total Fe to 0.1. LOI is Loss on Ignition. FeO is ferrous iron determined by titration methods. Alkalic Index = total alkali − (SiO2 × 0.37 − 14.43). Reference samples are in regular type and additional samples are in italics.

Table 3 (Representative Sample). Trace Element Analysis of Lavas Sampled by the HSDP-2 Core[a] (The full Table 3 is available in the HTML version of this article at http://www.g-cubed.org)

Sample ID	Run and Core Interval	Unit #	Depth, mbsl	Rock Type	Chem. Type	Nb, ppm	Zr, ppm	Y, ppm	Sr, ppm	Rb, ppm	Pb, ppm	Ga, ppm	Zn, ppm	Ni, ppm	Cr, ppm	V, ppm	Ce, ppm	Ba, ppm
SR0002-1.00	R2-1.0-2.0	1	−1.5	FL	ML	9.6	141	25.2	336	7.0	1	20	106	82	149	243	29	94
SR0008-0.30	R8-0.3-0.8	2	−8.8	FL	ML	8.8	130	23.3	333	6.3	1	19	100	112	309	246	25	85
SR0008-2.70	R8-3.4-4.2	2	−9.5	FL	ML	8.7	129	23.3	333	6.3	1	19	99	128	319	221	26	90
SR0018-0.10	R18-0.1-0.8	4	−25.7	FL	ML	7.3	106	19.2	244	4.8	2	15	100	560	721	207	20	59
SR0019-1.30	R19-1.3-1.9	5	−27.4	FL	ML	7.2	104	19.2	251	4.7	2	16	100	499	711	211	20	57
SR0022-4.30	R22-4.3-4.9	6	−33.1	FL	ML	7.1	103	18.9	248	4.7	1	16	98	514	779	200	19	66
SR0023-2.90	R23-2.90-3.60	6	−34.0	FL	ML	7.4	110	20.2	259	4.7	1	17	99	441	604	206	22	70
SR0028-2.20	R28-2.2-2.8	7	−41.6	FL	ML	5.4	84	15.2	183	3.8	1	13	94	831	1607	157	18	50
SR0031-0.50	R31-1.25-2.0	7	−45.5	FL	ML	3.3	52	10.2	134	2.0	1	9	93	1178	1864	119	11	35
SR0034-3.60	R34-3.6-4.5	8	−50.8	FL	ML	6.4	100	18.2	227	3.4	1	15	93	538	1408	180	19	61
SR0036-1.22	R36-2.1-2.9	8	−53.4	FL	ML	5.0	78	14.2	176	3.2	1	11	97	905	1723	149	16	53
SR0040-0.00	R40-0.0-0.9	9	−59.2	FL	ML	3.9	61	11.3	151	2.3	1	10	95	1062	1968	133	14	42
SR0040-1.07	R40-2.05-3.0	9	−59.5	FL	ML	4.2	68	12.2	149	2.8	1	10	95	1118	1940	128	16	46
SR0043-1.20	R43-1.2-1.8	11	−64.1	FL	ML	6.7	117	25.4	280	3.6	1	20	98	110	291	248	23	54
SR0046-1.15	R46-1.5-2.0	11	−68.8	FL	ML	6.9	119	25.5	277	3.3	2	19	100	110	292	258	22	60
SR0046-0.30	R46-0.3-0.8	12	−68.4	FL	ML	6.8	116	25.1	279	3.3	1	19	98	108	289	251	20	65
SR0049.03	R49-0.3-0.8	13	−72.9	FL	ML	8.1	131	24.6	295	4.5	1	20	95	99	348	227	22	67
SR0050-3.30	R50-3.3-3.8	14	−75.4	FL	ML	8.0	129	23.8	281	3.4	1	19	108	122	425	247	25	78
SR0054-0.1	R54-0.1-0.8	15	−79.9	FL	ML	7.9	125	24.4	278	2.4	1	19	106	133	428	251	21	52
SR0057-3.00	R57-3.75-4.5	15	−85.9	FL	ML	7.2	114	22.1	273	2.2	1	19	97	163	461	233	23	64
SR0059-4.10	R59-4.1-4.7	16	−89.4	FL	ML	7.5	120	22.7	281	3.7	2	19	92	122	415	199	23	69
SR0061-0.00	R61-0.65-1.30	16	−91.2	FL	ML	7.5	120	22.9	272	2.5	1	19	97	168	411	219	23	69
SR0066-4.10	R66-4.1-4.6	17	−100.1	FL	ML	4.3	62	11.4	123	0.4	1	10	102	1426	1461	151	15	31
SR0066-0.00	R67-0.40-1.30	18	−100.3	FL	ML	4.3	61	11.3	133	0.7	1	10	99	1438	1388	134	12	35
SR0070-4.50	R70-4.5-4.8	18	−106.3	FL	ML	6.6	95	17.6	214	1.9	1	14	103	721	1180	178	17	38
SR0073-0.00	R73-0.0-0.7	19	−109.5	FL	ML	7.9	119	22.5	270	4.7	1	19	94	162	468	211	22	66
SR0080-0.35	R80-1.22-2.0	19	−125.5	FL	ML	7.4	117	23.3	280	3.6	1	20	94	107	337	214	23	75
SR0083-7.10	R83-7.1-7.6	20	−136.8	FL	ML	8.0	128	24.5	287	2.3	1	20	95	111	337	228	27	71
SR0083-7.85	R83-8.50-9.20	20	−137.1	FL	ML	7.9	124	23.6	282	1.7	1	20	97	145	402	232	22	72
SR0085-1.10	R85-1.1-1.6	22	−141.1	FL	ML	6.9	107	22.8	264	0.5	1	21	91	123	242	230	20	72
SR0089-1.15	R89-1.15-1.85	22	−149.9	FL	ML	6.3	101	21.8	267	0.4	1	20	85	162	321	211	23	63
SR0093-6.55	R93-6.55-7.4	26	−163.3	FL	ML	8.3	123	23.8	267	0.1	1	21	105	115	374	234	26	92
SR0094-8.10	R94-8.1-8.6	26	−167.0	FL	ML	8.5	126	23.5	262	1.3	1	20	102	125	387	227	24	73
SR0098-2.00	R98-2.78-3.50	28	−177.8	FL	ML	6.1	86	15.9	193	3.0	1	13	100	1052	1081	169	14	42
SR0098-5.10	R98-5.1-5.7	28	−178.7	FL	ML	6.2	89	16.6	199	3.4	1	13	100	956	1070	177	16	44
SR0100-7.10	R100-7.1-7.7	29	−185.6	FL	ML	5.1	72	14.0	181	1.9	1	13	102	924	1096	168	15	47
SR0104-4.95	R104-5.75-6.50	32	−197.5	FL	ML	6.1	91	17.4	208	0.9	1	15	104	908	895	210	19	41

[a] Rock types: FL, subaerial flows; HY, hyaloclasties; MA, massive units; PI, pillows; IN, intrusives. Chem. Type, Chemical Type, i.e., ML is Mauna Loa, PS is Mauna Kea Post-Shield, MK-1 is Mauna Kea Type-1, MK-2 is Mauna Kea Type-2, MK-3 is Mauna Kea Type-3 and MK-4 is Mauna Kea Type-4.

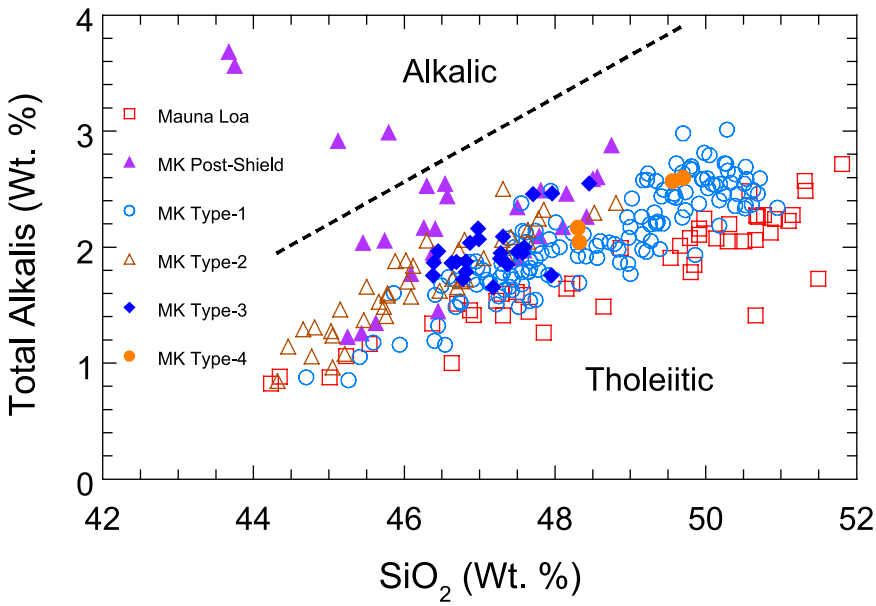

Figure 2. Total alkali silica diagram for lavas from HSDP-2. The dashed line separating alkalic from tholeiitic lavas is taken from *Carmichael et al.* [1974] and is given by total alkali = $SiO_2 \times 0.37 - 14.43$.

1995]. There is also a slight tendency for incompatible element ratios (Ba/Y, Sr/Y, Zr/Y) to decrease with increasing depth in the core (Figure 1). This is consistent with the observation that these ratios tend to decrease with increasing age in prehistoric Mauna Loa lavas [*Rhodes*, 1996; Rhodes, unpublished data]. In contrast with historical lavas, we do not observe significant changes in incompatible element ratios over narrow time intervals. This may reflect the fact that Mauna Loa lavas with high incompatible element ratios appear to be most common in the last 10 ka. Alternatively, it may simply be a sampling problem, a consequence of infrequent eruptions of about one flow every 2,500 years or so at the drill site [*Lipman and Moore*, 1996].

[14] Two samples of flow unit 22 are unusual for Mauna Loa lavas. At a given MgO content, they have much higher Al_2O_3 and correspondingly lower Fe_2O_3 contents than any other Mauna Loa lava sampled to date over a 300 ka eruptive history (Rhodes, unpublished data). In all other respects, this is a typical Mauna Loa lava. There is no petrographic or geochemical evidence (e.g., increased CaO or Sr) for plagioclase accumulation. On the basis of K_2O/P_2O_5, LOI and ferrous/ferric ratios, this flow unit is fairly extensively altered (M. J. Vollinger and J. M. Rhodes, Chemical alteration in basalts sampled by phase-2 of the Hawaii Scientific Drilling Project, manuscript in preparation, 2003), tempting attribution of its unique composition to alteration. On the other hand, lavas that show similar K_2O/P_2O_5, LOI and ferrous/ferric ratios from both Mauna Loa and Mauna Kea do not display comparably elevated Al_2O_3 values.

[15] In comparison with the underlying Mauna Kea tholeiites, the Mauna Loa lavas are slightly higher in SiO_2 and lower in CaO at a given MgO content, a characteristic of Loa versus Kea trend volcanoes [*Frey and Rhodes*, 1993; *Rhodes*, 1996]. However, there is considerable overlap. Some of the overlap in SiO_2 is due to alteration. It is now well established that Hawaiian lavas loose alkali elements (particularly K and Rb) and also SiO_2 as a consequence of weathering in wet tropical conditions [e.g., *Lipman et al.*, 1990; *Frey et al.*, 1990, 1994]. Such altered lavas are characterized by $K_2O/P_2O_5 < 1.4$, and often <1.0 [*Rhodes*, 1996]. In a companion paper (M. J. Vollinger and J. M. Rhodes, Chemical alteration in basalts sampled by phase-2 of the Hawaii Scientific Drilling Project, manuscript in preparation, 2003), we show that many of the HSDP basalts have $K_2O/P_2O_5 < 1.0$

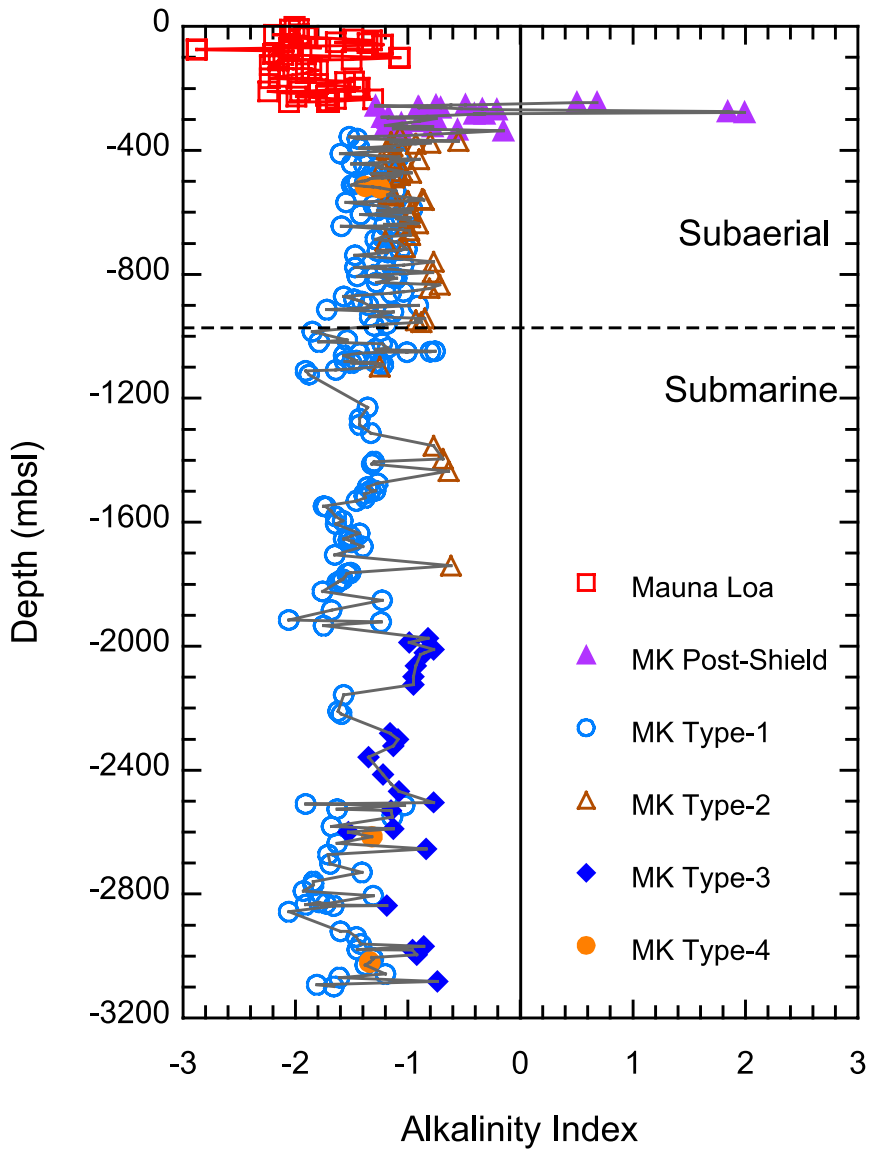

Figure 3. Variation of the alkalinity index with depth below sea level in samples from HSDP-2. The alkalinity index is a measure of the departure of a sample from the line separating alkalic from tholeiitic lavas in Figure 3 (alkalinity index = total alkali − (SiO_2 × 0.37 − 14.43).

and that for every 0.1 decrease in this ratio from around 1.4 the samples may have lost up to 0.13 wt.% SiO_2. Most other major and compatible trace elements are similar in abundance in tholeiites from the two volcanoes, as are abundances of Y and V. Incompatible element abundances, however, are consistently lower in Mauna Loa lavas (Figures 6 and 7). As noted above, incompatible trace element ratios involving Nb are characteristically lower (Figure 8) and prove useful discriminants. Similarly, ratios of Nb/Y, Ba/Y, Sr/Y, Zr/Y tend to be lower in Mauna Loa lavas than in Mauna Kea lavas (Figure 1).

4.2. Post-Shield Mauna Kea Lavas

[16] Tholeiitic basalts, constituting most of the Mauna Kea shield, are overlain by a thin sequence of inter-layered alkali basalts, transitional tholeiites, and tholeiitic basalts. These are the postshield lavas of the Hamakua Volcanics [*Frey et al.*, 1990; *Wolfe et al.*, 1997] that reflect the waning stages of volcanism on Mauna Kea. Post-shield lavas can be

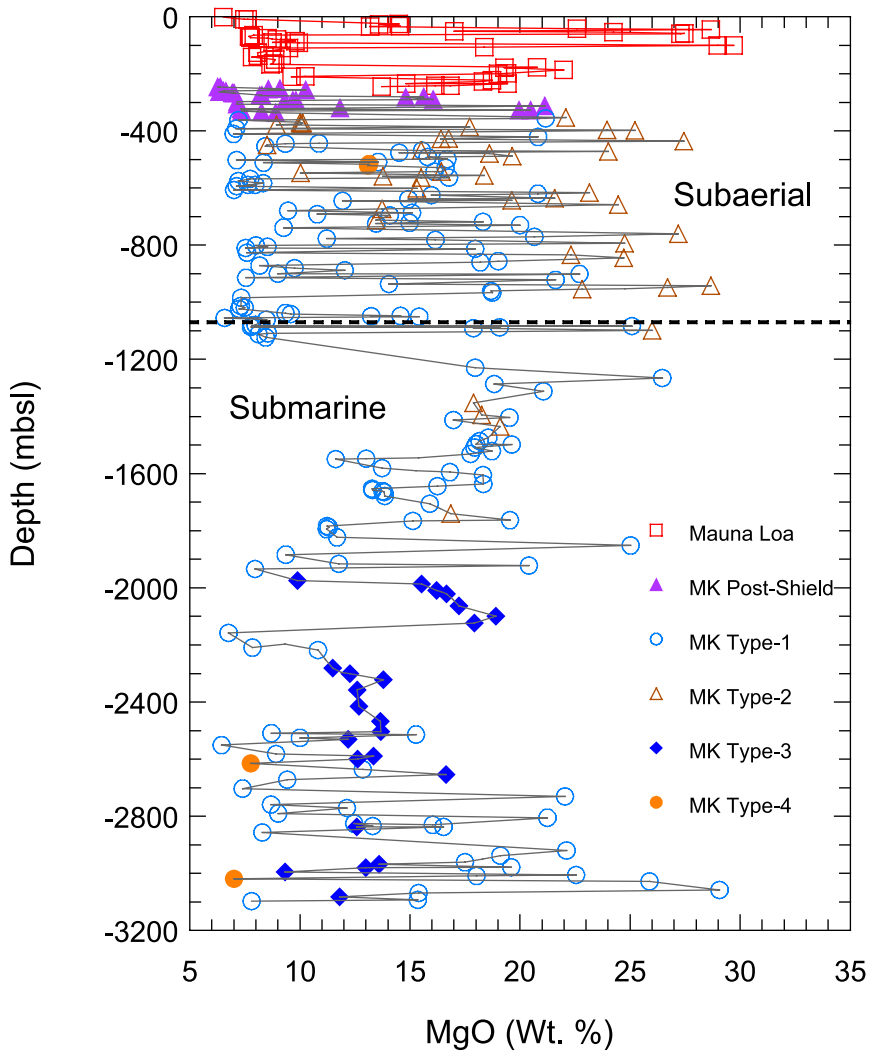

Figure 4. Variation of MgO content with depth below sea level in HSDP-2 lavas. Note the preponderance of low MgO subaerial lavas.

identified in the drill core immediately below the Mauna Loa lavas at 246 m (unit 42), down to a depth of 337 m (unit 63). Among this 107 m sequence of 23 flow units, only four analyses from units 42 and 48 reflect true alkali basalts (Figures 2 and 3). This contrasts with results from the pilot hole, where eight alkalic flows were identified [*Rhodes*, 1996]. *Huang and Frey* [2003] show that the alkali basalt of flow unit 48 is chemically identical to flow unit 58 in the pilot hole. Similarly, the other alkali basalt (unit 42) is close in composition to another alkali basalt (unit 51) in the pilot hole. Such correlations provide valuable means of relating age information from the two drill cores [*Sharp et al.*, 1996; Sharp et al., submitted manuscript, 2003]. The alkali basalts are distinctly lower in SiO_2 and higher in TiO_2, total iron as Fe_2O_3, V and Y as well as most incompatible elements than other Mauna Kea tholeiites at a corresponding MgO content (Figures 5–8).

[17] The remaining 21 flow units assigned to the postshield lavas include both transitional tholeiites and regular tholeiites. The transitional tholeiites are characterized by one or more of the following characteristics: high total alkalis at a given SiO_2 content, with alkalinity indices between zero and −0.6 (Figures 2 and 3); lower

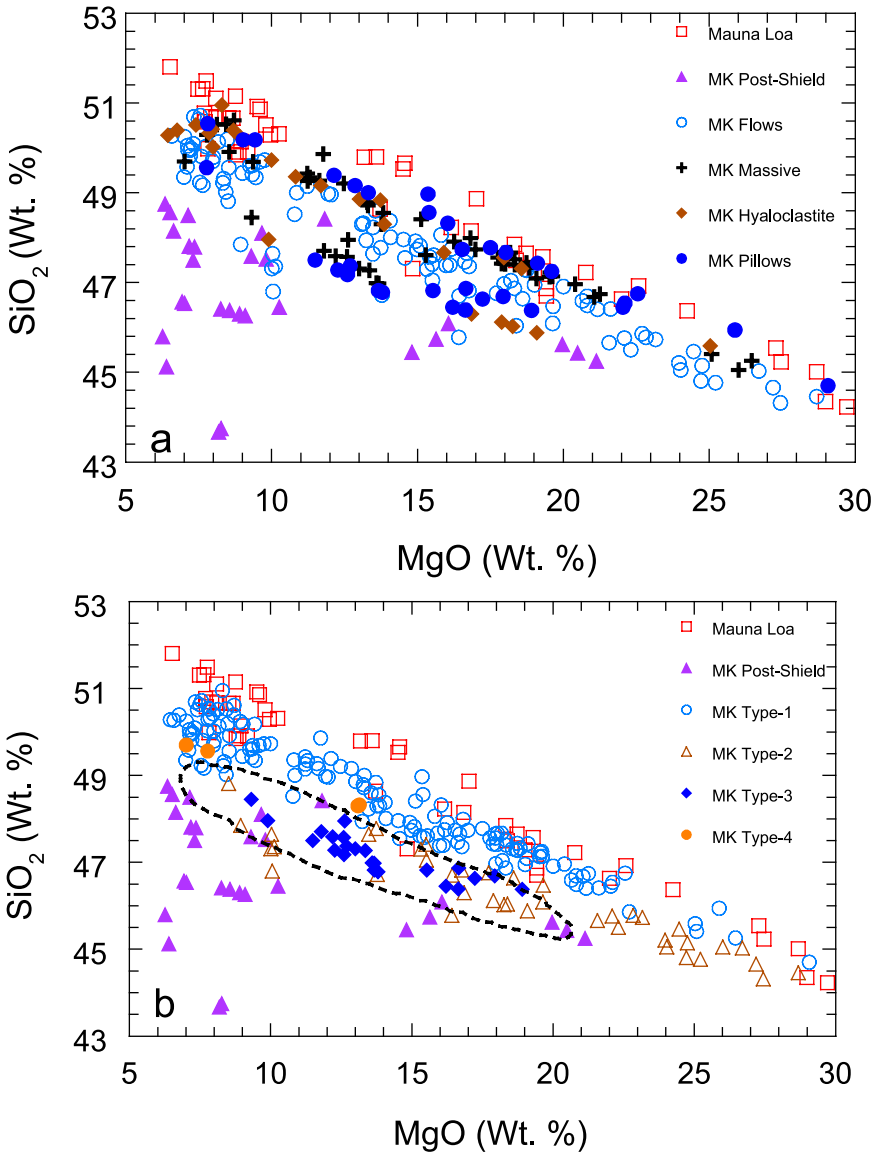

Figure 5. Abundance of SiO_2 versus MgO content in lavas from HSDP-2. In Figure 5a the Mauna Kea samples are plotted according to lithological types and in Figure 5b according to magma types. See text for more details on the classification of Mauna Kea tholeiites into magma types. The field for Loihi tholeiites is shown by the dashed line.

SiO_2 and higher TiO_2, Sr, Ba and Nb than other Mauna Kea tholeiites at a given MgO content (Figures 5–8); and total iron as Fe_2O_3 greater than 13.5% (Figure 6b). In comparison with regular Mauna Kea tholeiites, they also tend to have higher ratios of TiO_2/Al_2O_3, Ba/Y, Nb/Y and Zr/Y (Figure 1). The regular tholeiites inter-layered with the alkali basalts and transitional tholeiites do not differ significantly in composition from tholeiites lower in the subaerial section of the drill core. They are included with the postshield lavas simply because they are inter-layered with them and were erupted during the same period. It must be emphasized, however, that the cut-off of the postshield lavas at unit 63 at a depth of 337 m is arbitrary. As we will discuss below, there are low-SiO_2 tholeiites below 337 m, with chemical characteristics that are similar to the tholeiites inter-layered with the transitional tholeiites and alkali basalts of the postshield lavas. *Huang and Frey* [2003] have classified these low-SiO_2 tholeiites as post shield

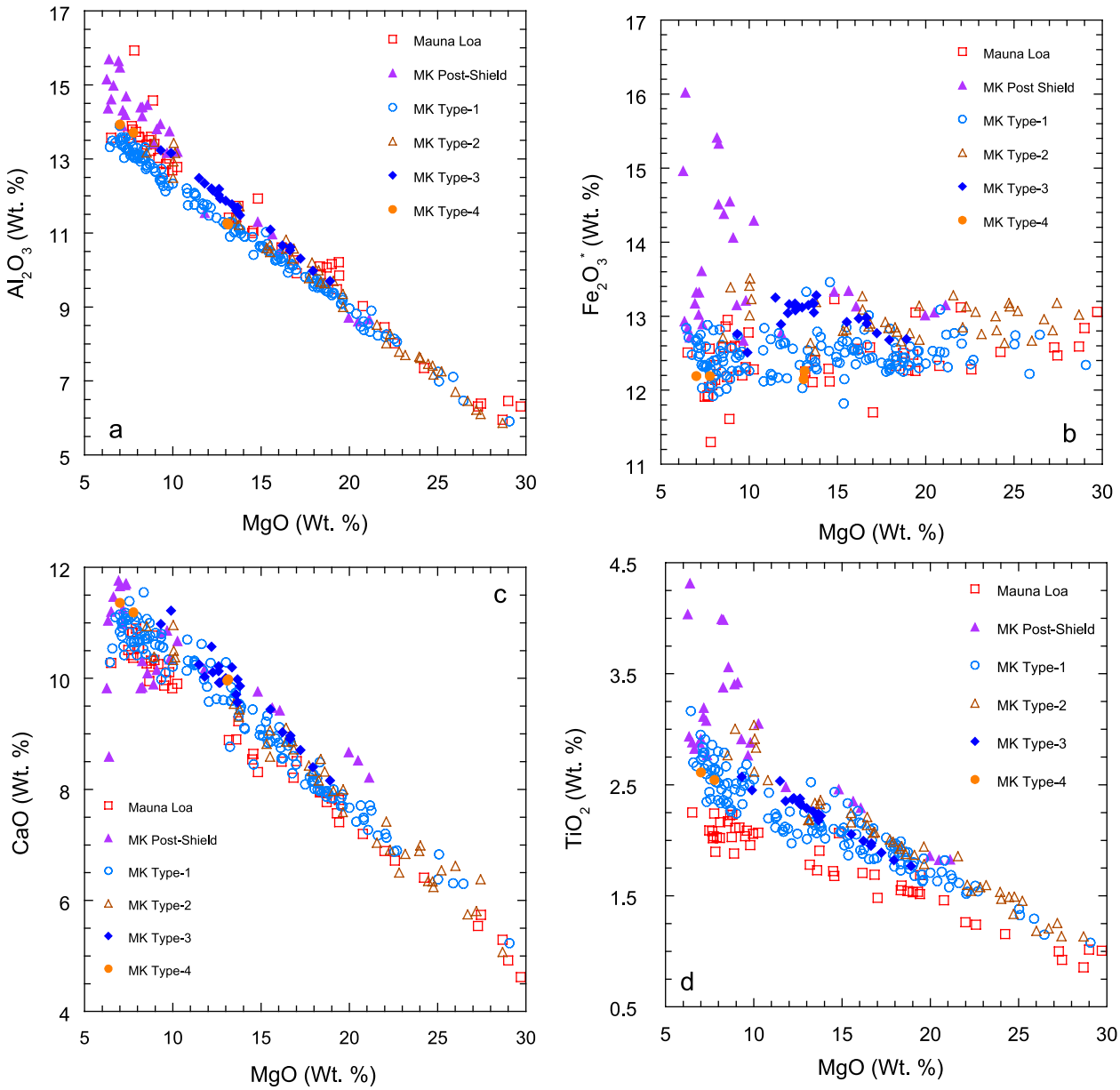

Figure 6. Abundances of major elements (a) Al_2O_3, (b) total iron as Fe_2O_3, (c) CaO, and (d) TiO_2 versus MgO content in lavas from HSDP-2.

lavas, thereby extending the transition from shield to post shield lavas to a greater depth in the core.

4.3. Mauna Kea Tholeiites

[18] Below 337 m (unit 66) to the bottom of the core at 3098 m (unit 345) all the lavas are tholeiitic (Figures 2 and 3). All have alkalinity indices between −0.6 and −2.0, and total iron as Fe_2O_3 is less than 13.5% (Figure 6b). There are no further inter-layered alkalic basalts or transitional tholeiites. Subaerial Mauna Kea tholeiitic lava flows extend to a depth of 1079 m (flow unit 168) and overlie submarine pillow lavas, hyaloclastites and massive and intrusive units [*Seaman et al.*, 2000]. There are no obvious differences in composition for these various eruptive types: all overlap in compositional trends with MgO, as is clearly evident in Figure 5a. The Mauna Kea tholeiites exhibit a wide range in MgO, from

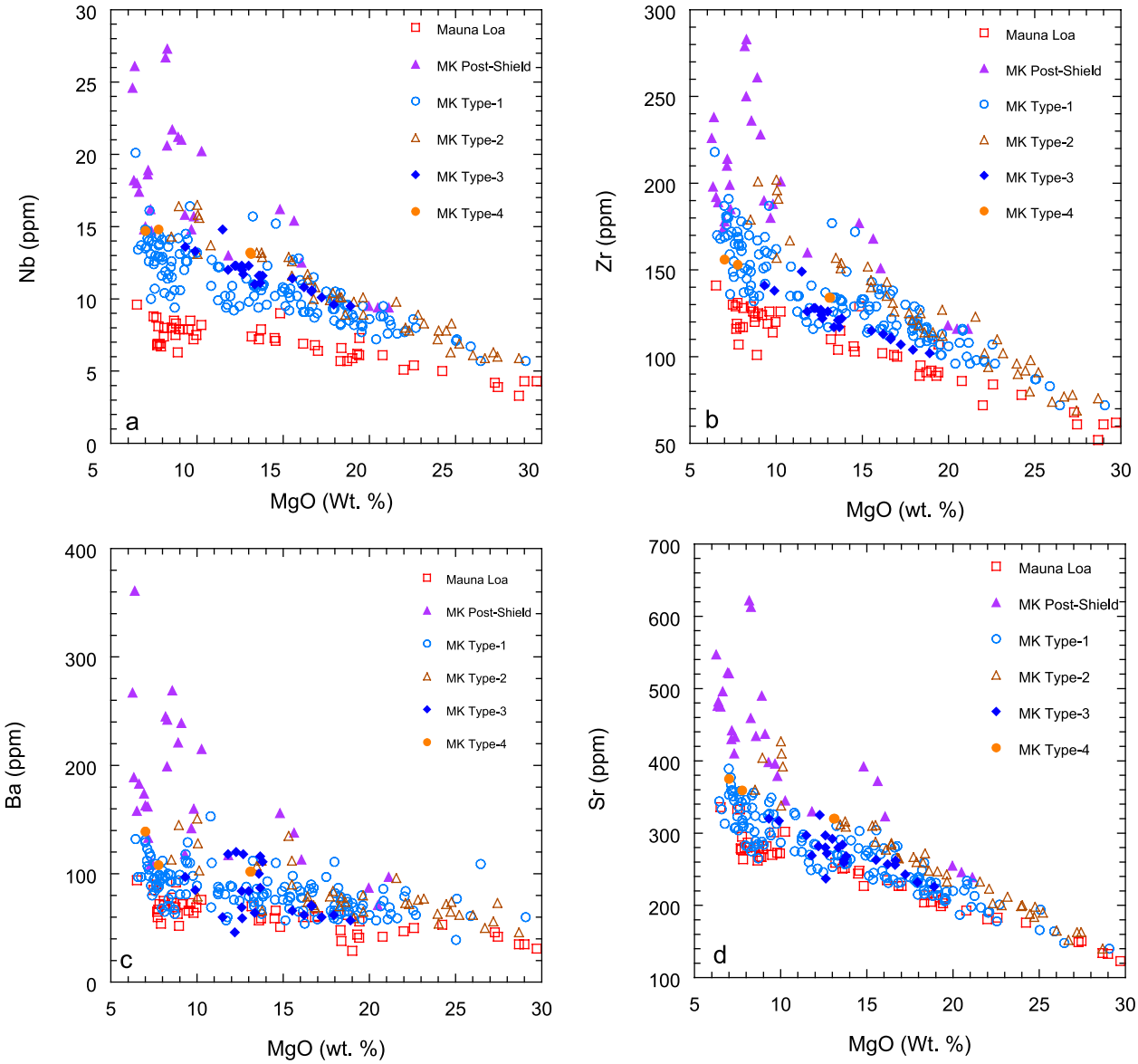

Figure 7. Abundances of trace elements (a) Nb, (b) Zr, (c) Ba, and (d) Sr versus MgO content in lavas from HSDP-2.

6.4 to 29.1 wt.%. As with the Mauna Loa tholeiites, there is a bi-modal distribution in MgO content (Figures 4–6): one group with lower MgO contents between 6.4–10 wt.%, and a picritic group with more than 13 wt.% MgO. This is particularly evident in the subaerial lavas, where there is a distinct hiatus between 10 to 13 wt.% MgO. The hiatus in the submarine lavas between 10 and 11 wt.% is less pronounced. The high and low MgO groups are not uniformly distributed throughout the core. The picrites are common throughout both the subaerial and submarine sections. The lower MgO group are most prevalent in the subaerial section of the core, and less abundant below 1079 m in the submarine section (Figure 4).

[19] When compared with the overlying Mauna Loa tholeiites, the Mauna Kea tholeiites tend to be lower in SiO_2 and higher in total alkalis, TiO_2, and CaO, as well as most incompatible elements, at a corresponding MgO content (Figures 5–7). With the exception of TiO_2 and Nb, there is, however, some overlap between the two volcanoes for most of these elements. In contrast

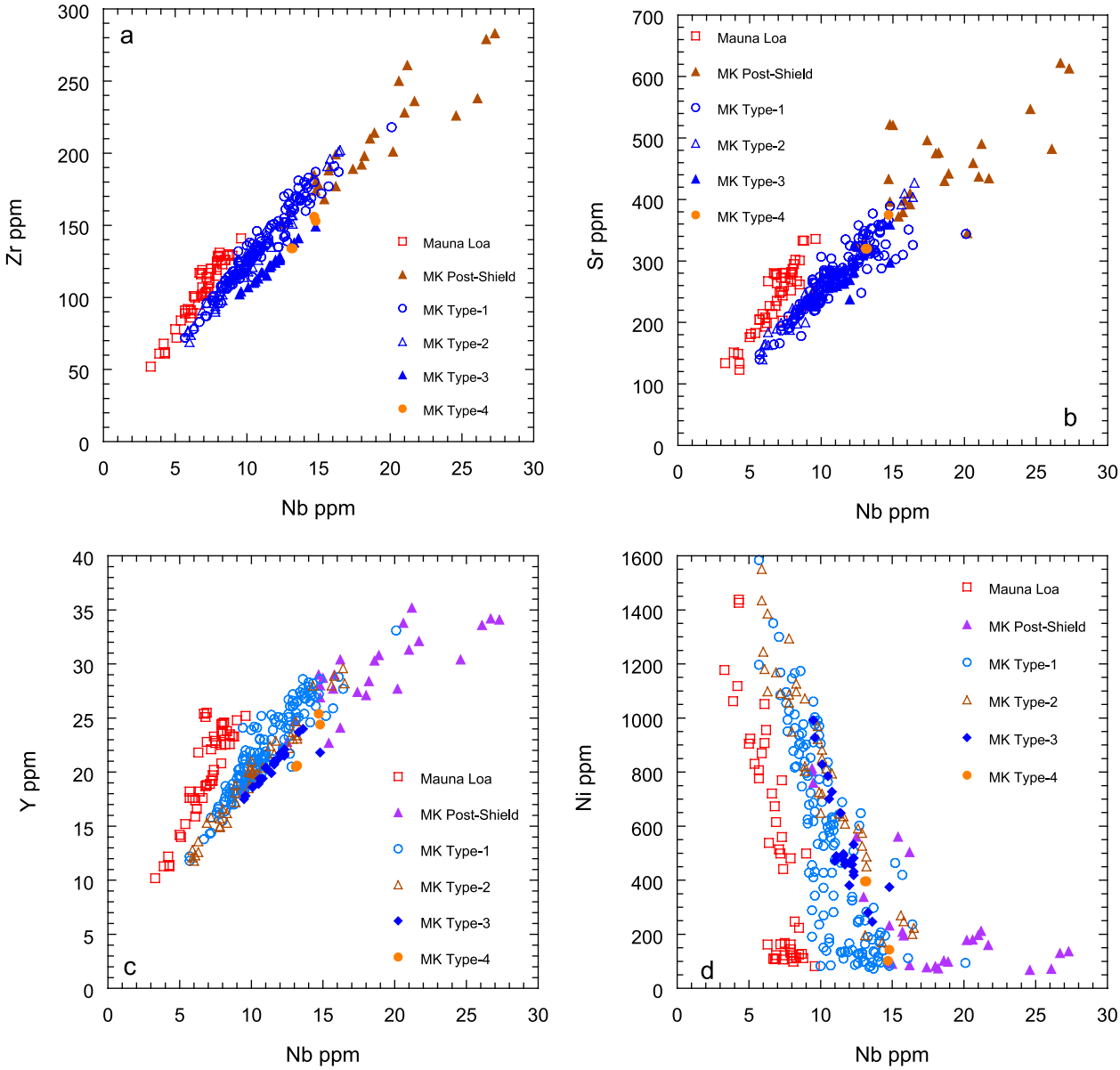

Figure 8. Abundances of trace element (a) Zr; (b) Sr; (c) Y, and (d) Ni versus Nb in HSDP-2 lavas.

with the Mauna Loa tholeiites, there is a greater scatter in most elements at a given MgO value (Figures 5–7). The coherence of Mauna Loa data appears to be a fundamental characteristic when compared with other Hawaiian volcanoes, especially those on the Kea trend [*Frey and Rhodes*, 1993; Rhodes, unpublished data]. This scatter is particularly evident for SiO_2 (Figure 5). There are lavas with SiO_2 values as much as 1.0 to 1.5 wt.% lower, at a corresponding MgO content, than the more "normal" Mauna Kea tholeiites. In part, this may be a consequence of loss of SiO_2 through alteration. However, many of the low-SiO_2 tholeiites are quite fresh, with normal K_2O/P_2O_5 ratios of about 1.4 to 1.7, and E. M. Stolper, S. Sherman, M. Garcia, M. B. Baker, and C. Seaman (Glass in the submarine section of the HSDP2 drill core, Hilo, Hawaii, manuscript submitted to *Geochemistry Geophysics Geosystems*, 2003, hereinafter referred to as Stolper et al., submitted manuscript, 2003). report glass data with a similar range in SiO_2 values. To help clarify the range in SiO_2 at a given MgO content, the SiO_2 data has been normalized to a constant

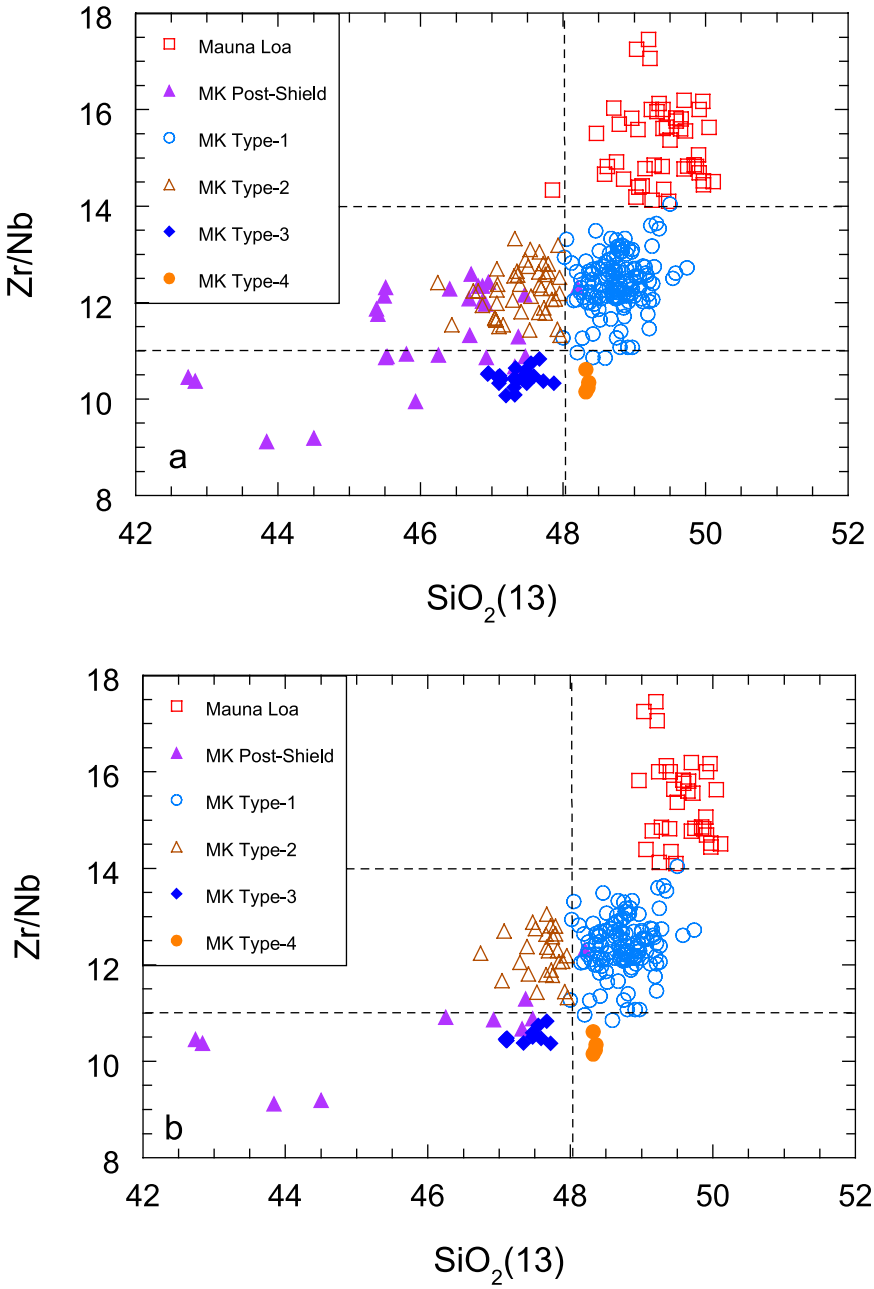

Figure 9. Variation of $SiO_2(13)$ and Zr/Nb in HSDP-2 lavas. This figure illustrates the rationale behind the classification of Mauna Kea tholeiites into four magma types. See text for more details. $SiO_2(13)$ is calculated from the equations in Table 4. All samples are plotted in Figure 9a, whereas in Figure 9b samples have been screened for alteration by plotting only samples with $K_2O/P_2O_5 > 1$.

MgO of 13 weight% by adding or subtracting olivine (Fo_{89}) plus 2% Cr-spinel. The composition of the olivine and spinel are based on analyses reported by *Garcia* [1996]. Such a simple procedure is warranted because almost all of the tholeiites are on, or close to, olivine-control trends, and very few have less than 7% MgO, or show evidence of fractionation involving clinopyroxene or plagioclse. The normalized $SiO_2(13)$ values exhibit a wide range from 46.5–49.7%. Lavas with $SiO_2(13)$ values between 48–49% SiO_2 are typical of the vast majority of Mauna Kea tholeiites analyzed to date, whereas those with lower values have not previously been

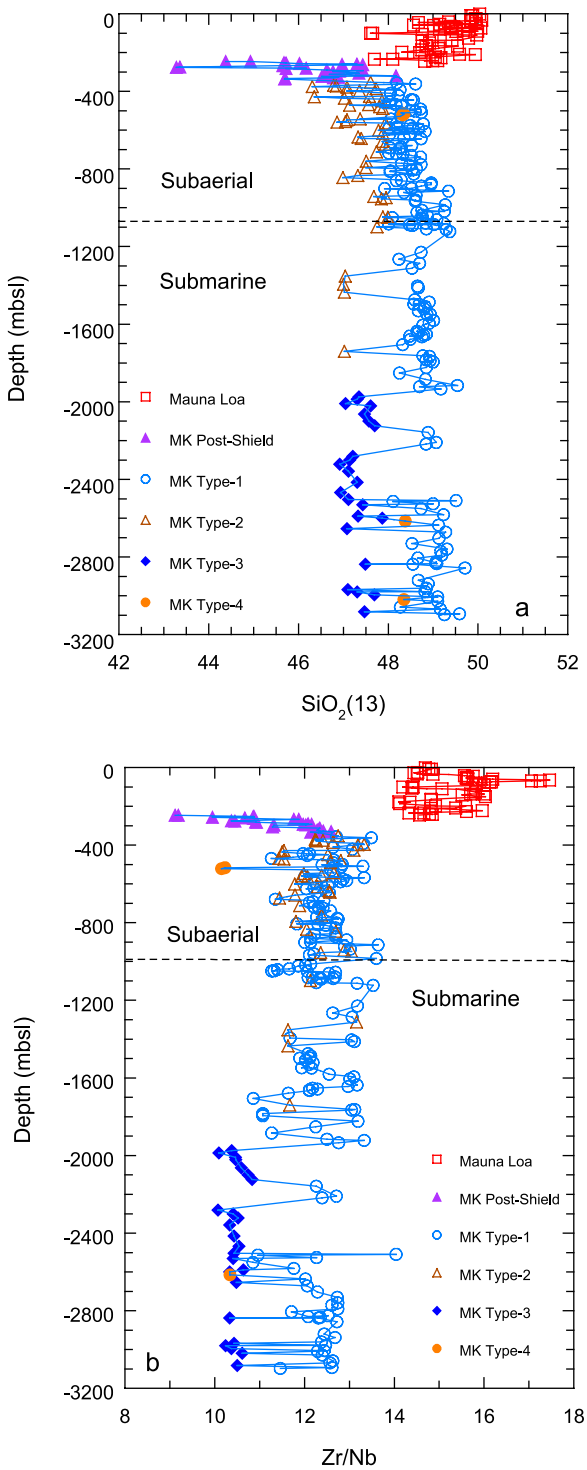

Figure 10. Variation of $SiO_2(13)$ and Zr/Nb with depth below sea level in HSDP-2 lavas. This figure illustrates the distribution of the Mauna Kea magma types with depth.

recognized on Mauna Kea [*Frey et al.*, 1990, 1991; *Rhodes*, 1996; *Wolfe et al.*, 1997].

[20] To assist in further discussion of the magmatic stratigraphy and evolution of Mauna Kea volcano, we have subdivided the tholeiitic lavas into four magma types based on normalized SiO_2 values ($SiO_2(13)$) and on Zr/Nb ratios (Figure 9). It should be emphasized that this distinction is somewhat arbitrary, and that these four tholeiitic magma types are not entirely discrete: there are overlapping and intermediate compositions. Additionally, some samples have undoubtedly lost SiO_2 through alteration and may be mis-classified. Nonetheless, we consider it a valuable exercise with useful petrogenetic implications.

[21] Type-1 Magmas (145 samples) are defined as tholeites and picrites having normalized SiO_2 values between 48–50%, and Zr/Nb ratios between 11 and 13. Additionally, although there is considerable overlap, type-1 magmas tend to have lower alkalinity indices (Figure 3) and somewhat lower abundances of incompatible elements at a given MgO than the other three magma types (Figures 6–7). Total iron content also tends to be slightly lower than in magma types 2 and 3, but comparable to type 4 (Figure 6b). Despite slightly lower incompatible element abundances, with the exception of ratios involving Nb, the range for ratios such as Ba/Y, Zr/Y and Sr/Y is comparable to the ranges found for these ratios in the other magma types (Figure 1). The type-1 magmas display well-developed, coherent linear compositional trends over a wide range in MgO content (Figures 5–7) from 6.4 to 26.5 percent. There is, however, a paucity of samples between 9.5 and 12 percent. Only two samples (units 165 and 305) display evidence, such as low MgO accompanied by low CaO/Al_2O_3, of multiphase fractionation, beyond olivine control.

[22] Lavas corresponding to the type 1 magmas were erupted as subaerial flows, pillow lavas, hyaloclastites and massive units (Figure 5). They are present throughout the entire tholeiitic section of the drill core, from just below the postshield lavas at 356 m to the bottom of the hole at 3098 m (Figure 10). They constitute about 60% of the

Mauna Kea lavas analyzed from the drill core to date. Type-1 lavas correspond with previously described Mauna Kea tholeiites [*Frey et al.*, 1990, 1991; *Rhodes*, 1996] and with the high-SiO_2 glass group recognized by Stolper et al. (submitted manuscript, 2003) in the HSDP-2 core.

[23] Type-2 Magmas (42 samples) have Zr/Nb between 11–13, comparable to values in the type-1 magmas. They are distinguished from the type-1 magmas by lower normalized SiO_2 values between 46.2 and 48% (mostly between 47–48%). It must be emphasized, however, that the boundary between the two magma types at 48% SiO_2(13) is somewhat arbitrary; there is complete gradation between the type-1 to type-2 lavas (Figure 9). Alkalinity indices, total iron content, and incompatible element abundances at a fixed MgO content are slightly higher than in the type-1 magmas. The lavas corresponding to type-2 magmas also exhibit well-defined, coherent, compositional trends with MgO. The range in MgO from 8.5 to 28.7 percent is similar to that of the type-1 lavas (Figures 5–7), but there are more picrites (>12% MgO). Unlike the Mauna Loa lavas and type-1 Mauna Kea lavas, there is no cluster of compositions around 7–8% MgO. In many respects the type-2 lavas resemble the tholeiites that are inter-layered with the post-shield alkalic basalts and transitional tholeiites between 246 and 337 m. Given that the only significant difference between type-1 and type-2 magmas is in the SiO_2 content, it is pertinent to ask how much of this difference is a consequence of alteration. Figure 9 compares all of the data, with data that have been screened for alteration ($K_2O/P_2O_5 > 1$). Although the numbers of type-2 samples are reduced, it is clear that there are a significant number with SiO_2(13) below 48%. The 20 least altered of the type-2 lavas ($K_2O/P_2O_5 > 1.0$) have an average SiO_2(13) value of 47.53% compared with an average for the group as a whole of 47.33%, whereas the average for the type-1 lavas is 48.69%. A few type-1 lavas have undoubtedly been misclassified as type-2 lavas because of loss of SiO_2 through alteration. For example, there are pairs of samples from type-1 units 83, 94 and 105 where the most altered of the pairs (lower K_2O/P_2O_5) have SiO_2(13) values below 48%.

[24] Type-2 lavas constitute about 17% of the analyzed Mauna Kea samples. In contrast with the type-1 lavas, type-2 lavas are restricted to the upper part of the Mauna Kea section, where they are inter-layered with the type-1 lavas. They are most abundant in the subaerial section (Figure 10), and are extremely abundant between 337 and 850 m, constituting about 40% of all the lavas sampled in that interval. Below 850 m they constitute only 10% of the sampled lavas, becoming increasingly rare with depth. The lowest type-2 lava in the core is flow unit 243, a hyaloclastite, at a depth of 1739 m. Re-examination of the pilot hole data shows that type-2 lavas were present in that core also, although they were not distinguished from type-1 lavas at the time [*Rhodes*, 1996].

[25] Type-3 Magmas (23 samples) have normalized SiO_2 values between 46.9 and 48%, similar to the type-2 magmas. They also have similar alkalinity indices (Figures 2 and 3), and are clearly not alkalic as stated by some authors [e.g., *Blichert-Toft et al.*, 2003]. They differ from the type-2 magmas in that Zr/Nb are lower: between 10–11. This is because, although Nb abundances at a given MgO content are similar to the type-2 magmas, Zr abundances are considerably lower (Figures 7–8). They also tend to be on the high side of the Mauna Kea tholeiite range in total iron, CaO, Al_2O_3 and TiO_2 at a fixed MgO content (Figure 6). In many respects, the compositional characteristics of the type-3 tholeiites are close to tholeiites from Loihi volcano (Figure 5b) [*Garcia et al.*, 1993, 1995b; *Rhodes*, 2000]. Zr/Nb is characteristically low, and they have very similar abundances of SiO_2, CaO, total iron at a given MgO content. The major differences between these and Loihi tholeiites are in Al_2O_3 and TiO_2, which are slightly higher. The range in MgO content for lavas corresponding to the type-3 magmas, from 9.3 to 18.9%, is more restricted than for types 1 and 2. This may, in part, be due to the smaller number (23) of samples. They do, however, form a coherent group displaying strong linear compositional trends with MgO (Figures 5–7).

[26] Lavas corresponding to the type-3 magmas, which constitute about 9% of the analyzed Mauna Kea core, are found only in the submarine section

of the core, inter-layered with type-1 lavas between 1974 and 3098 m. The first occurrence down the core is just above the uppermost sequence of pillow lavas (Figure 10). They tend to occur as packages of associated pillow lavas, hyaloclastites and massive units. They correspond very closely with the low-SiO_2 glasses identified by Stolper et al. (submitted manuscript, 2003) below 1950 m.

[27] Type-4 Magmas (4 samples) are similar to type-1 magmas having normalized SiO_2 values above 48%. Their total iron contents are also low, in common with the type-1 magmas (Figure 6b). The major characteristic that distinguishes them from the type-1 magmas is that they tend to have higher Nb and Sr abundances at a given MgO content (Figure 7). This results in Zr/Nb of less than 11 (Figure 9), and high Nb/Y and Sr/Y, similar to the type-3 magmas (Figure 8). Lavas corresponding with type 4 magmas are very rare in the section (Figure 10). There are two samples of flow unit 92: high in the subaerial section at a depth of 516 m, and submarine flow units 310 and 341 at depths of 2615 and 3019 m respectively. Unit 310 is a pillow, whereas 341 is a massive unit. Because of the few samples, the range in MgO content is not large, from 7.0 to 13.1 percent. Nonetheless, they do appear to form a coherent compositional group.

5. Discussion

5.1. Parental Magmas and Magmatic Processes

5.1.1. Mauna Kea Post-Shield Lavas

[28] The postshield lavas are a diverse, highly scattered group that, unlike the other Mauna Kea lavas, does not define coherent trends with MgO (Figures 5–7). Part of this diversity is due to alteration: only 10 of the 28 samples have $K_2O/P_2O_5 > 1$ (Figure 9). Part is due to crystal fractionation and mixing beyond olivine control. Several of the low-MgO lavas have high TiO_2 and total iron, accompanied by low CaO and CaO/Al_2O_3 ratios indicative of clinopyroxene fractionation. Others with high MgO, but with high total iron and low CaO, may be mixed magmas. Plots of Nb-Ni (Figure 8d) confirm that many of these lavas have fractionated beyond olivine control, and Nb-V relationships suggests that fractionation may even have been sufficiently extensive to involve crystallization of opaque minerals.

5.1.2. Mauna Loa and Mauna Kea Tholeiites

[29] The Mauna Loa lavas and the four Mauna Kea magma types form remarkably well-defined linear compositional trends when plotted against MgO (Figures 5–7). This is especially true for the Mauna Loa and Mauna Kea type-1 and -2 lavas. They extend from as low as 6.5–7.0% MgO to as much as 27–30% MgO. The type-3 and -4 Mauna Kea lavas are more restricted in range, from 9.3 to 18.9% MgO and from 7.0 to 13.1% MgO respectively, possibly a consequence of fewer samples of these two types. These linear trends converge toward olivine compositions and are indicative of the strong influence of olivine accumulation and fractionation [e.g., *Powers*, 1955; *Murata and Richter*, 1966; *Basaltic Volcanism Study Project*, 1981; *Wilkinson and Hensel*, 1988; *Clague et al.*, 1995; *Rhodes*, 1995]. Assuming that olivine fractionation accompanies olivine accumulation, the resulting trends should be curvi-linear, not straight, a consequence of changing olivine compositions with change in melt compositions and decreasing temperatures. For most major element trends, the anticipated curvature is not large and only becomes discernible from linear trends at low MgO values. Fortunately, this is not the case for MgO–FeO relationships (Figure 11). Crystallization of olivine ranging from Fo_{91} to Fo_{82} in Hawaiian tholeiites with MgO contents between 18 to 7 percent MgO results in a markedly curving decrease in FeO with decreasing MgO. Below 7% MgO, olivine begins to react with the melt to produce pigeonite, accompanied by plagioclase and clinopyroxene crystallization [*Helz and Thornber*, 1987; *Montierth et al.*, 1995], resulting in a rapid increase in FeO with little further loss in MgO (Figure 11). The glass data follow this fractionation trend [*Garcia*, 1996; Stolper et al., submitted manuscript, 2003], presumably in response to cooling and crystallization after the lavas are erupted. The whole rock data, however, do not. They remain essentially linear to

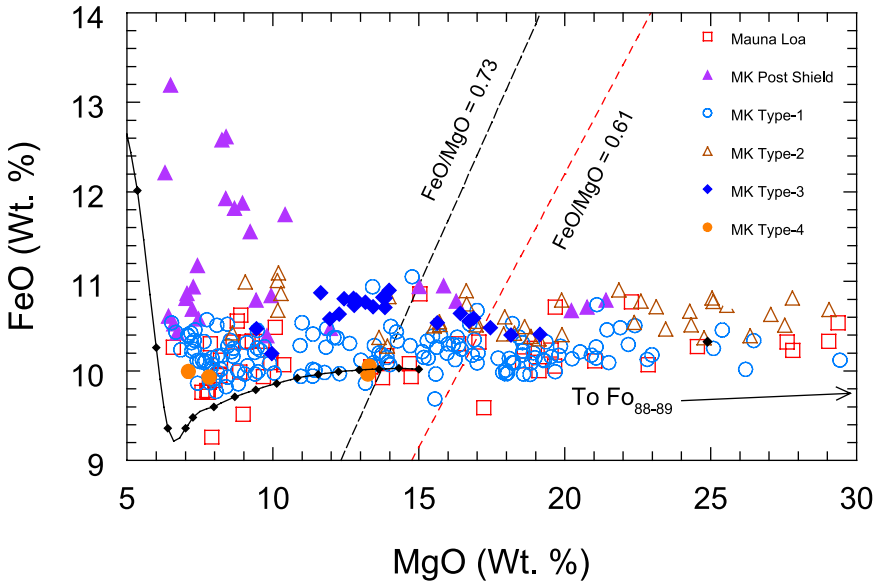

Figure 11. FeO versus MgO in HSDP-2 lavas. FeO is calculated from total iron by assuming that 10% of the iron is present as Fe^{3+}. The two oblique dashed line represent the FeO/MgO ratio of melts in equilibrium with Fo_{89} (black) and Fo_{91} (red) olivine respectively (assuming $K_D = 0.3$ [*Roeder and Emslie*, 1970]). The intersection of these lines with the data provides an estimate of the MgO content of the parental, and possible primary, Mauna Loa and Mauna Kea magmas from which Fo_{89} and Fo_{91} olivine crystallized. Also shown are an accumulation trend for Fo_{88-89} olivine and the liquid line of descent for a parental Mauna Loa magma with 15% MgO. The liquid line of descent is based on the 1 atm. experiments of *Montierth et al.* [1995] and glass data of *Garcia et al.* [1995a].

the low MgO end of the trends at about 6.5–7.0% MgO. This point is emphasized further in a plot of Ni versus Nb (Figure 8d), where an olivine fractionation trend should be curved in response to rapidly decreasing Ni $kd^{olivine/melt}$ with decreasing melt temperature and MgO content [*Hart and Davis*, 1978; *Kinzler et al.*, 1990]. There can be little doubt that these linear trends are mixing and not fractionation trends, possibly resulting from the accumulation of olivine in low MgO (6.5–7.0%) magmas. For example, *Clague et al.* [1995] attribute the linear trends in the whole rock data from Kilauea's submarine Puna ridge to entrainment of an olivine cumulate mush (average composition $Fo_{87.9}$) in a later, unrelated, differentiated, low-MgO magma. However, this cannot be the entire story, other processes must be at work. If olivine accumulation were the only factor, then the intersection of each of the regression lines of major oxides and trace elements versus MgO should intersect olivine compositions with a common forsterite content, corresponding to the average accumulated olivine in each of the magma types [*Maaløe*, 1979; *Clague et al.*, 1995]. This is not the case. Regression equations of SiO_2, TiO_2, Al_2O_3, FeO and CaO and several incompatible trace elements versus MgO for the five magma types are given in Table 4. Also listed are olivine compositions, calculated from the intersection of these equations with the compositional range for olivine. Only unaltered samples, with $K_2O/P_2O_5 > 1$, were used to calculate the equations and olivine compositions. Note that for each magma type, the calculated olivine composition varies widely. For example, all five magma types extrapolate to olivine compositions close to Fo_{89} for FeO-MgO, but to quite different and variable forsterite content (Fo_{79-99}) for other oxides and trace elements. *Clague et al.* [1995] noted a similar inconsistency for the Puna Ridge data. Regression of MgO versus FeO yielded an extrapolated olivine composition of $Fo_{87.9}$, consistent with the average olivine composition, whereas regression of MgO versus Ni resulted in a much lower value of $Fo_{84.7}$. The problem is worse for the incompatible trace elements. Linear trends with MgO (Figure 7) tend to converge at high values of MgO and, in some cases, actually cross. Again, the calculated olivine

Table 4. Regression Data, Calculated Olivines and MgO(13) Values[a]

Variable	Equation	Calc. Fo	13% MgO
	Mauna Loa		
SiO_2	53.363 − 0.2921 * MgO	85.7	49.57
TiO_2	2.593 − 0.0589 * MgO	82.9	1.83
Al_2O_3	16.446 − 0.3677 * MgO	84.3	11.67
FeO	9.973 + 0.0116 * MgO	89.1	10.12
CaO	12.417 − 0.2490 * MgO	89.9	8.79
Nb	9.498 − 0.1803 * MgO	95.0	7.2
Zr	148.884 − 3.0041 * MgO	90.8	109.8
Ba	85.383 − 1.6871 * MgO	92.3	63.5
Sr	350.793 − 7.5008 * MgO	87.1	253.3
Y	28.889 − 0.6109 * MgO	87.8	20.9
	Mauna Kea Type-1		
SiO_2	52.048 − 0.2580 * MgO	86.4	48.69
TiO_2	3.122 − 0.0693 * MgO	84.4	2.22
Al_2O_3	15.828 − 0.3446 * MgO	85.9	11.35
FeO	10.159 + 0.0033 * MgO	89.3	10.20
CaO	12.919 − 0.2603 * MgO	89.6	9.54
Nb	15.871 − 0.3596 * MgO	83.6	11.2
Zr	195.784 − 4.4231 * MgO	83.7	138.3
Ba	116.407 − 2.3950 * MgO	89.6	85.3
Sr	394.745 − 8.9199 * MgO	83.7	278.8
Y	31.537 − 0.7005 * MgO	84.7	22.4
	Mauna Kea Type-2		
SiO_2	50.029 − 0.1924 * MgO	90.0	47.53
TiO_2	3.594 − 0.0884 * MgO	78.6	2.44
Al_2O_3	16.234 − 0.3627 * MgO	84.4	11.52
FeO	10.473 − 0.0048 * MgO	88.9	10.41
CaO	13.251 − 0.2794 * MgO	82.3	9.62
Nb	19.895 − 0.5148 * MgO	76.2	13.2
Zr	239.843 − 6.1308 * MgO	76.8	160.1
Ba	144.763 − 3.2959 * MgO	83.3	101.9
Sr	495.922 − 12.6133 * MgO	77.1	331.9
Y	35.687 − 0.8524 * MgO	80.5	24.6
	Mauna Kea Type-3		
SiO_2	49.966 − 0.1985 * MgO	88.7	47.39
TiO_2	3.313 − 0.0817 * MgO	75.5	2.25
Al_2O_3	16.771 − 0.3755 * MgO	84.2	11.89
FeO	10.518 − 0.0022 * MgO	89.0	10.49
CaO	14.001 − 0.3088 * MgO	84.1	9.99
Nb	17.832 − 0.4468 * MgO	77.9	12.0
Zr	180.132 − 4.2438 * MgO	81.3	125.0
Ba	145.282 − 4.4837 * MgO	67.8	87.0
Sr	393.232 − 8.6993 * MgO	85.0	280.1
Y	29.589 − 0.6414 * MgO	86.2	21.3
	Mauna Kea Type-4		
SiO_2	51.329 − 0.2301 * MgO	88.2	48.34
TiO_2	3.087 − 0.0688 * MgO	84.1	2.19
Al_2O_3	16.609 − 0.3919 * MgO	81.1	11.51
FeO	9.910 − 0.0074 * MgO	89.4	9.81
CaO	12.959 − 0.2279 * MgO	99.1	10.00
Nb	16.779 − 0.2759 * MgO	>100	13.2
Zr	180.993 − 3.5838 * MgO	92.1	134.4
Ba	154.568 − 4.0788 * MgO	75.2	101.5
Sr	428.816 − 8.3215 * MgO	93.5	320.6
Y	30.565 − 0.7647 * MgO	78.0	20.0

[a] Equations were calculated from samples with $K_2O/P_2O_5 > 1$.

compositions are highly variable (Table 4). This should not happen if only olivine accumulation and fractionation are involved. Clearly, there is considerable uncertainty in extrapolating these trends to olivine compositions, and this may explain some of the differences in the calculated average forsterite contents. A full statistical treatment is needed, but is beyond the scope of this paper. Two examples are presented, however, to illustrate the problem. In the Mauna Loa lavas the calculated olivine compositions at the 95% confidence level for MgO versus CaO and MgO versus Al2O3 are $Fo_{89.9\pm0.63}$ and $Fo_{84.3\pm0.49}$ respectively. Similarly, the calculated olivine compositions in the type-1 Mauna Kea tholeiites for MgO versus CaO and MgO versus Al2O3 are $Fo_{89.6\pm0.69}$ and $Fo_{85.9\pm0.24}$. Clearly, these differences in the calculated olivine compositions are real, and not simply a consequence of uncertainty in extrapolating the data.

[30] The relationship between CaO and Al_2O_3 (Figures 12a and 12b) helps to clarify this problem. Mauna Loa and Mauna Kea olivines contain negligible amounts of Al_2O_3 and a small amount of CaO which increases with decreasing forsterite content from about 0.18 to 0.37 [e.g., *Garcia*, 1996]. In Figure 12a the trends for each of the magma types are very similar, and all extrapolate to CaO contents that are much too high (>0.6%) for any reasonable olivine composition. Addition of 1–2% of Cr-spinel to the accumulating olivine does not solve these problems. It helps with SiO_2 and TiO2, but not FeO or CaO. Also, if only olivine fractionation or accumulation were involved, there should be no change in CaO/Al_2O_3 with MgO. Figure 12b shows that this is not the case: all of the magma types exhibit a decrease in CaO/Al_2O_3 with decreasing MgO. To explain these trends, mixing of magmas with differing CaO/Al_2O_3 values is required, in addition to the accumulation or entrainment of olivine.

[31] *Maaløe* [1979] discussed this problem for Hawaiian tholeiites in general. He concluded that the well-defined linear trends so characteristic of Hawaiian tholeiites were not a consequence of olivine accumulation and fractionation, but of mixing two distinct primary magmas, one with MgO of about 10% and the other with about

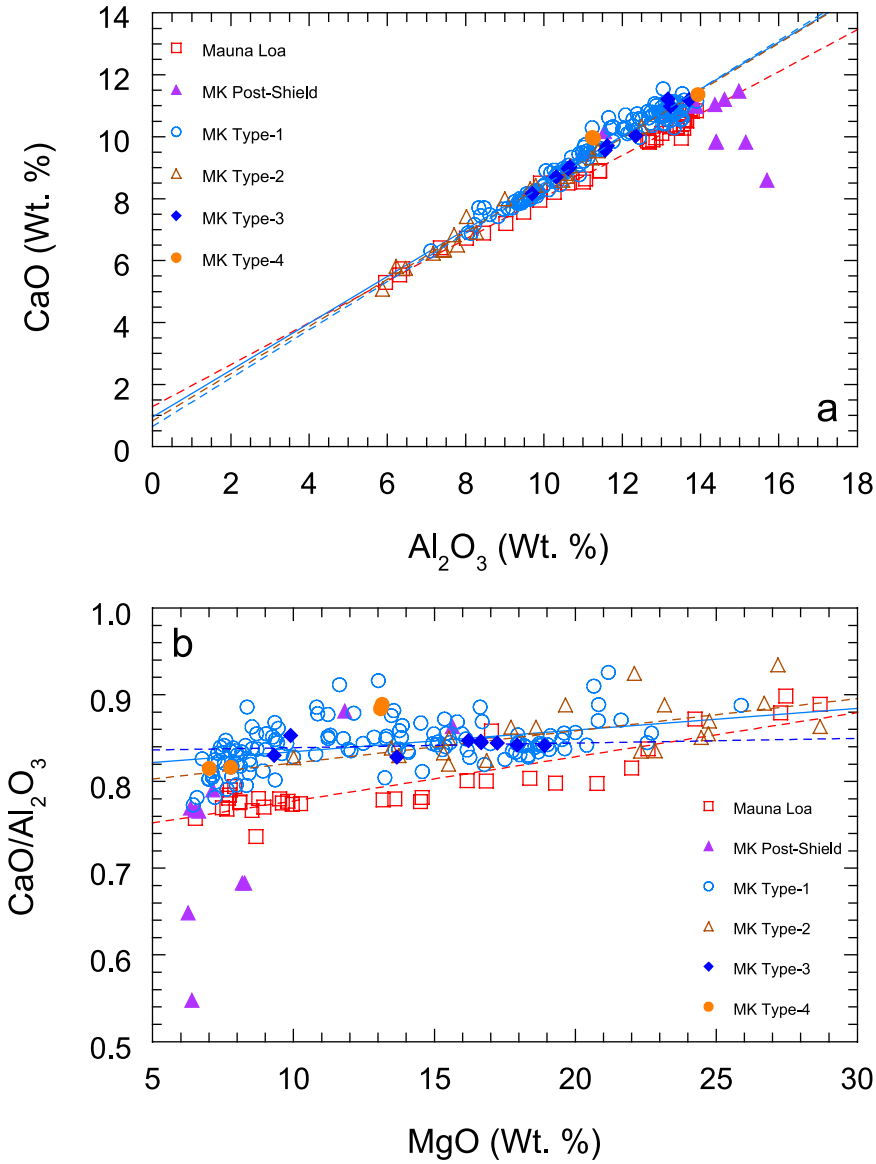

Figure 12. Variations in (a) CaO versus Al_2O_3 and (b) CaO/Al_2O_3 vesrsus MgO in HSDP-2 lavas. The data have been screened for alteration by removing samples with $K_2O/P_2O_5 < 1$. In Figure 12a the intersection of the regression lines with the abscissa for the different magma types are all too high for reasonable olivine compositions. In Figure 12b the CaO/Al_2O_3 ratios of all of the tholeiites decrease with decreasing MgO. This should not happen if the trends result solely from olivine fractionation, accumulation or entrainment.

20%. This seems to us like throwing the baby out with the bath water! For a start, the process of olivine accumulation in Hawaiian tholeiites has been too thoroughly documented using olivine–whole rock relationships to be lightly discarded [e.g., *Murata and Richter*, 1966; *Wilkinson and Hensel*, 1988; *Garcia et al.*, 1995a; *Clague et al.*, 1995; *Rhodes*, 1995; *Baker et al.*, 1996; *Garcia*, 1996]. In general, lavas with Mg-values greater than about 0.71–0.75 (corresponding to about 14–18% MgO) have whole rock compositions that are too high in MgO to be in equilibrium with their olivine phenocrysts. They have undoubtedly accumulated some olivine and are unlikely to reflect melt compositions. Secondly, the high MgO ends of the trends for both Mauna Loa and Mauna Kea lavas are almost 30% MgO. These are improbable candidates for parental end-member magmas, even for proponents advocating picritic compositions [e.g., *Macdonald*, 1968; *Maaløe*, 1979; *Wright*,

1984; *Clague et al.*, 1991; *Garcia et al.*, 1995a; *Rhodes*, 1995, 1996]. What, then, is the explanation for these remarkably linear trends that approach, but fail to intersect with, appropriate and consistent olivine compositions? The answer, we believe, lies in a combination of mixing of distinct magmas accompanied by olivine accumulation or entrainment. At one end of the trends are MgO-rich parental magmas laden with up to 40% of accumulated or entrained olivine, and at the other end are low-MgO magmas with around 7% MgO. The composition of the high-MgO magmas can be reasonably well established. As noted earlier, there is a distinct hiatus in MgO content between about 10 and 13 percent in the Mauna Loa and Mauna Kea type-1 tholeiites. This provides a low limit of around 13% MgO for the proposed high-MgO magma, similar to the estimate of parental magma composition for historical Mauna Loa and Kilauea picrites [*Wilkinson and Hensel*, 1988; *Rhodes*, 1995]. The high MgO end of the range can be estimated from olivine phenocryst compositions. The most abundant high-forsterite olivines in these lavas are around Fo_{89} [*Garcia et al.*, 1995a; *Garcia*, 1996; *Baker et al.*, 1996; Putirka, personal communication, 2002]. Some of these are xenocrysts, but others are most certainly phenocrysts, and according to *Garcia* [1996] there is no significant difference in composition between phenocrysts and xenocrysts. Olivine phenocrysts of Fo_{89} have crystallized from picritic melts with Mg-values of around 0.71 and FeO/MgO ratios of about 0.73 (assuming a K_D of 0.3 ± 0.03 [*Roeder and Emslie*, 1970]). For Mauna Loa and Mauna Kea magmas, the intersection of this ratio with the MgO-FeO regression lines corresponds to MgO contents of 13–15 percent (Figure 11). This estimate is similar to submarine picritic glasses from Kilauea described by *Clague et al.* [1991] that most certainly reflect liquid compositions. Although these are the most probable candidates for the high-MgO parental magmas involved in mixing in the volcanic plumbing system, it is unlikely that they represent primary magmas. Occasional olivine phenocrysts as forteritic as $Fo_{90.7}$ have been reported from both Mauna Loa and Mauna Kea lavas [*Garcia et al.*, 1995a; *Garcia*, 1996; *Baker et al.*, 1996]. Applying the same reasoning as above, this implies that primary magmas for the two volcanos could have FeO/MgO around 0.61, and MgO contents as high as 17–18% MgO (Figure 11); similar to the estimates of *Clague et al.* [1995] for Kilauea.

[32] The low-MgO end of the mixing trend is less tractable. *Maaløe* [1979] addressed this problem by proposing that in addition to Hawaiian primary magmas with around 20% MgO, there were also primary melts with around 10% MgO or less. Mixing between these magmas was responsible for the linear Hawaiian tholeiitic arrays. Alternatively, Takahashi and coworkers [*Takahashi et al.*, 1993, 1998; *Kogiso et al.*, 1998] have argued that Hawaiian primary magmas are not picritic, but low-MgO tholeiites, produced by melting of eclogite blobs in peridotitic plume material. The role of eclogite (or garnet pyroxenite) as a source of magma in the Hawaiian plume is controversial. Several workers have proposed that eclogite is the source of the high- SiO_2 Koolau magmas [*Hauri*, 1996; *Lassiter and Hauri*, 1998; *Takahashi et al.*, 1998; *Takahashi and Nakajima*, 2002] and therefore a source component for Loa trend volcanoes. On the other hand, *Stracke et al.* [1999] argue that trace and isotopic data are inconsistent with eclogite as a source component of any tholeiitic Hawaiian magmas. More recently, melting experiments of *Takahashi and Nakajima* [2002] show that, if eclogite pods melt together with garnet peridotite the resultant melts will be picritic (because of the buffering effects of olivine in the surrounding peridotite). Only if the eclogitic melt can be isolated from the plume peridotite will low-MgO primary magmas be produced. In passing we note that the proposed linear mixing trends are characteristic of all four Mauna Kea magma types, as well as the Mauna Loa magmas. This means that if eclogite melting is the source of the low-MgO magmas, then eclogite is a necessary source component of both Loa and Kea trend volcanoes.

[33] We believe that there is a simpler, more petrologically appealing explanation for the almost ubiquitous presence of low-MgO magmas that mix with picritic magmas. Hawaiian tholeiitic magmas with MgO at around 7% are at the low-MgO end of olivine control trends, and are multiply saturated

with olivine, pigeonite, plagioclase and clinopyroxene [*Wright and Peck*, 1978; *Helz and Thornber*, 1987; *Montierth et al.*, 1995]. In a closed system, with decreasing temperature and continuing differentiation, olivine will react with the magma to produce pigeonite before multiphase fractionation can continue, leading to FeO and TiO_2 and incompatible element enrichment and a corresponding decrease in CaO, Al_2O_3 and CaO/Al_2O_3. In an open system, however, continual or intermittent replenishment by a more primitive, MgO-rich magma will pull the mixed magma composition back into the olivine field, resulting in quasi steady state magmas "perched" at or close to the end of the olivine-control trend [*Rhodes*, 1988, 1995; *Rhodes and Hart*, 1995]. The MgO contents of these magmas will vary with magma supply rates [*Defant and Nielson*, 1990]. In summary, we suggest that the well-defined linear trends are mixing trends involving low-MgO, quasi "steady state" magmas with more primitive melts containing about 14–15% MgO that are laden with olivine phenocrysts and xenocrysts. Figure 12b provides a test of this suggestion. If olivine accumulation and fractionation are the only processes involved, then CaO/Al_2O_3 should remain constant over the entire range in MgO. If, however, quasi "steady state" magmas are involved in the mixing process, then CaO/Al_2O_3 should decrease with decreasing MgO because of crystallization of pyroxene and plagioclase in the "steady state" magma. This is clearly the case, especially for the Mauna Loa lavas. Additionally, we wish to observe that if our interpretation is correct, and of general application, the common practice of back-calculating to putative primary magma compositions through addition of incremental amounts of equilibrium olivine, may well lead to incorrect results and spurious correlations with MgO.

[34] If one examines the MgO content of the lavas with stratigraphic depth (Figure 4), a number of interesting points emerge. The low-MgO Mauna Loa lavas increase in MgO content from around 7.5% to 8–9% with increasing depth. The simplest explanation is that the magma supply rate is increasing with increasing age, with the consequence that the quasi "steady state" magmas are more effectively pulled into the olivine field [*Defant and Nielsen*, 1990]. In the case of the Mauna Kea lavas, there are abundant type-1 lavas, with around 7% MgO, from immediately below the postshield lavas at 356 m. down to around 1100 m just below the subaerial/submarine transition. There are no more low-MgO lavas, of any magma type, below this depth until around 2100 m. Below this, they are present again, but are relatively uncommon (Figure 4). We believe this to be an important observation, reflecting a fundamental change at about 440 ka (DePaolo et al., manuscript in preparation, 2003) in Mauna Kea's magmatic plumbing system. Two explanations, both related to magma supply rate, come to mind. The first is that a continuously replenished magma chamber, in which "steady state" magmas could evolve, did not develop on Mauna Kea until late in its history, after around 440 ka. This suggestion is counterintuitive, because the very idea of continuously replenished magma chambers is thought to be a consequence of robust magma supply [e.g., *O'Hara*, 1977; *Rhodes et al.*, 1979; *Rhodes*, 1988; *Defant and Nielsen*, 1990]. Alternatively, prior to 440 ka, although a continuously replenished magma chamber was in existence, magma supply rates may have been sufficiently high that the "steady state" magmas were not low in MgO. The model depth-age curve of DePaolo et al. (manuscript in preparation, 2003) gives some credence to this idea. Prior to the transition from submarine to subaerial lavas at a depth of 1080 m, the estimated lava accumulation rate is between 15–21 mm/yr, with an average of about 18 mm/yr. The estimated lava accumulation rates for the subaerial lavas are much less than this, declining from about 5 mm/yr to about 2.8 mm/yr below the transition to postshield lavas.

5.2. Origin and Evolution of Mauna Kea Magmas

[35] There are considerable, and fluctuating, variations in the composition of Mauna Kea lavas, especially in SiO_2 content and Zr/Nb, throughout the 2852 m. cored interval (Figure 10). Indeed, it is on the basis of these variables that we have identified four tholeiitic magma types, beneath the postshield Hamakua lavas. Experimental studies

have shown that melting of peridotite produces magmas with SiO_2 contents that are sensitive to the depth of melting and melt segregation and, to a lesser degree, to the extent of melting [*Hirose and Kushiro*, 1993; *Kushiro*, 1996; *Kogiso et al.*, 1998; *Longhi*, 2002]. Additionally, trace element ratios involving Nb (e.g., Zr/Nb, K/Nb, Nb/Y) correlate with isotopic ratios in Hawaiian shield lavas, and therefore also reflect changes in source components [*Rhodes et al.*, 1989; *Frey and Rhodes*, 1993; *Frey et al.*, 1994; *Rhodes*, 1996; *Rhodes and Weis*, 2001]. The implications are that, over the 400 ka or so of eruptive history recorded by the drill core (DePaolo et al., manuscript in preparation, 2003), there may have been perceptible shifts in melt production, depth of melting and melt segregation, and in the proportions of plume source components.

5.2.1. Magma Source

[36] The isotopic data for Hawaiian shield-building tholeiites is widely interpreted in terms of melting of mixtures of two end-member mantle plume components [e.g., *Staudigal et al.*, 1984; *West et al.*, 1987; *Frey and Rhodes*, 1993; *Lassiter and Hauri*, 1998]. One component, with high $^{87}Sr/^{86}Sr$ and low $^{206}Pb/^{204}Pb$ and $^{143}Nd/^{144}Nd$ is best characterized by lavas from Koolau volcano; the other component, with low $^{87}Sr/^{86}Sr$ and high $^{206}Pb/^{204}Pb$ and $^{143}Nd/^{144}Nd$, is represented by lavas from Kilauea volcano. A third component, most clearly identified in Loihi lavas, is required to account for high $^{3}He/^{4}He$ in some lavas [*Kurz et al.*, 1995] and for high $^{208}Pb/^{204}Pb$ relative to $^{206}Pb/^{204}Pb$ [*Staudigal et al.*, 1984; *Garcia et al.*, 1995b; *Eiler et al.*, 1998]. As noted above, trace ratios involving Nb correlate with these isotopic ratios, and also reflect changes in the source components. Zr/Nb is particularly useful in this respect because it is less susceptible to changes associated with melting than other ratios (e.g., Figure 13a). High Zr/Nb is associated with the Koolau component, whereas low Zr/Nb is characteristic of the Kilauea and Loihi components. Clearly, then, the large differences in Zr/Nb and Nb/Y between Mauna Loa and Mauna Kea lavas (Figures 1, 8–10, and 13) provide not only useful discriminants between lavas from the two volcanoes, but also provide evidence that their magmas come from distinctly different plume sources. The source(s) of the Mauna Kea lavas are closest to the Kilauea and Loihi components, whereas the Mauna Loa source is intermediate between the Koolau and Kilauea end-members. This assertion is well established [e.g., *Frey and Rhodes*, 1993] and is amply backed by recent isotopic data from the Hawaii Scientific Drilling Project [*Hauri et al.*, 1996; *Lassiter et al.*, 1996; *Blichert-Toft et al.*, 2003; J. Bryce and D. DePaolo, High resolution Sr and Nd isotopic records of Mauna Kea volcano: Results from the second phase of the Hawaii Scientific Drilling Project (HSDP-2), manuscript in preparation, 2003].

[37] The majority of Mauna Kea lavas, that is, types-1 and 2, have similar and overlapping Zr/Nb and Nb/Y ratios (Figures 1, 8–10, and 13), suggesting that they are derived from a common plume source. Again, isotopic data is consistent with this interpretation [*Blichert-Toft et al.*, 2003; Bryce and DePaolo, manuscript in preparation, 2003]. Although there are subtle fluctuations in the Hf, Sr, Nd and Pb isotopic ratios for these lavas throughout the core, there are no major or systematic changes indicative of significant changes in the proportion of plume components. The type-3 and 4 lavas are another matter. Their X/Nb ratios differ clearly from those of the type-1 and 2 lavas, with lower Zr/Nb and higher Nb/Y (Figures 1, 8–10, and 13). These ratios cannot be explained away as a consequence of less melting than the type-1 and 2 magmas. This is evident from plots of Zr/Nb versus Sr/Y and Zr/Y versus Nb/Y (Figure 13) where the type- 3 and 4 lavas plot separately from the other Mauna Kea tholeiites. A hypothetical incremental melting curve for a garnet peridotite primitive mantle [*Norman and Garcia*, 1999] is shown for reference, to illustrate the trajectories taken by melting curves in these diagrams. It is clear that the type-3 and 4 lavas are not produced by melting of the same source as other Mauna Kea lavas. As noted earlier, the type-3 lavas have many close similarities, both in major and trace elements, with tholeiites from Loihi volcano, and must be melts from a source that differs from that of the other Mauna Kea lavas. The isotopic data are

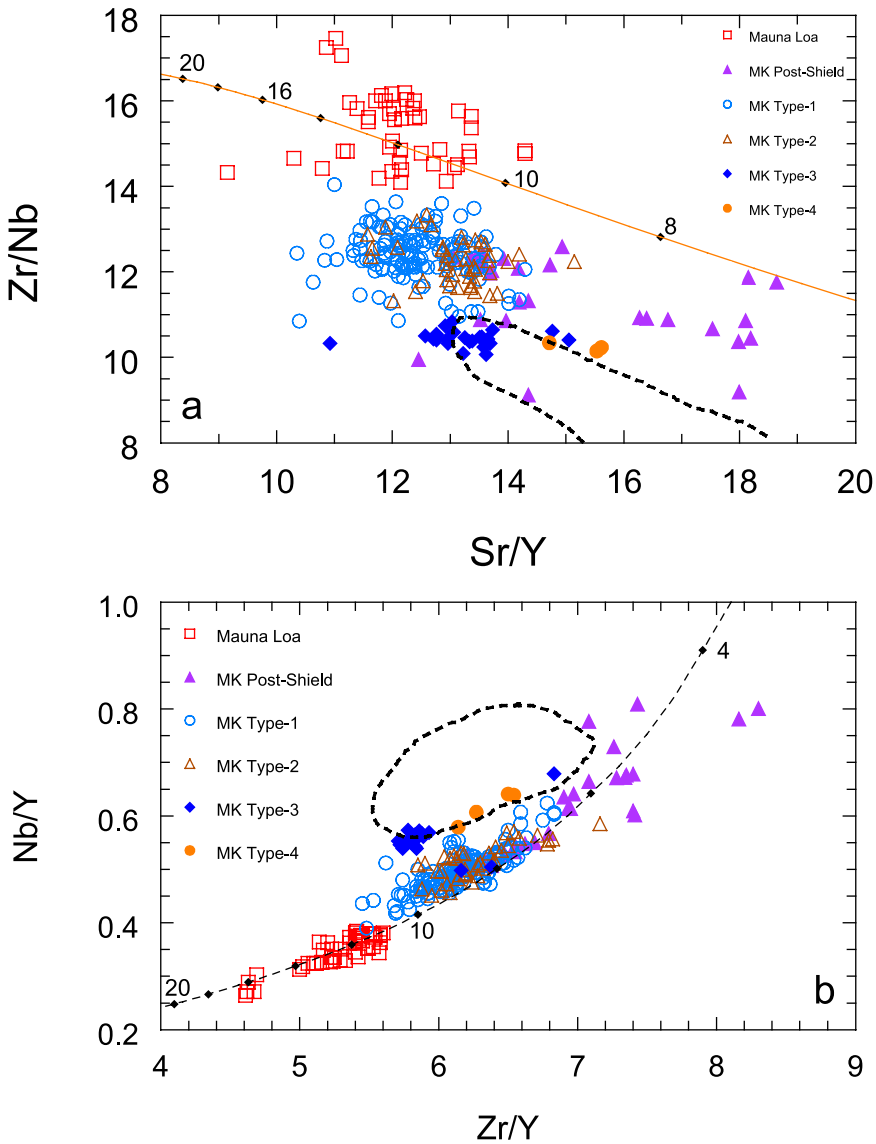

Figure 13. Incompatible element abundance ratios in HSDP-2 lavas. (a) Zr/Nb versus Sr/Y and (b) Nb/Y versus Zr/Y. Shown for reference are accumulated incremental melting curves for a garnet lherzolite primitive mantle [*Norman and Garcia*, 1999]. See text for further discussion. The field for Loihi tholeiites is shown by the dashed line.

more equivocal on this issue [*Blichert-Toft et al.*, 2003; Bryce and DePaolo, manuscript in preparation, 2003]. There is little significant difference in the isotopic ratios of Sr, Pb, Nd and Hf between the low Zr/Nb type-3 and 4 lavas and the higher Zr/Nb type-1 and 2 lavas (Figure 14). Although overlapping with the type-1 and 2 lavas, the type-3 and 4 lavas tend to fall at the isotopic extremes of the range (Figure 14). In contrast, there are real differences in $^{3}He/^{4}He$ and in $^{208}Pb/^{204}Pb$ relative to $^{206}Pb/^{204}Pb$ [M. D. Kurz, J. Curtis, D. Lott, and A. Solow, Rapid Helium isotope variability in Mauna Kea shield lavas from the Hawaii Scientific Drilling Project, manuscript submitted to *Geochemistry, Geophysical, Geosystems*, 2003, hereinafter referred to as Kurz et al., submitted manuscript, 2003; *Blichert-Toft et al.*, 2003]. This is illustrated in Figure 14, where $^{3}He/^{4}He$ and $\Delta 8/4$ Pb values (relative to the northern hemisphere reference line [*Hart*, 1984]) are plotted against Zr/Nb. Both tend to be higher in the type-3 lavas, along with Zr/Nb, again indicating close similarity with Loihi tholei-

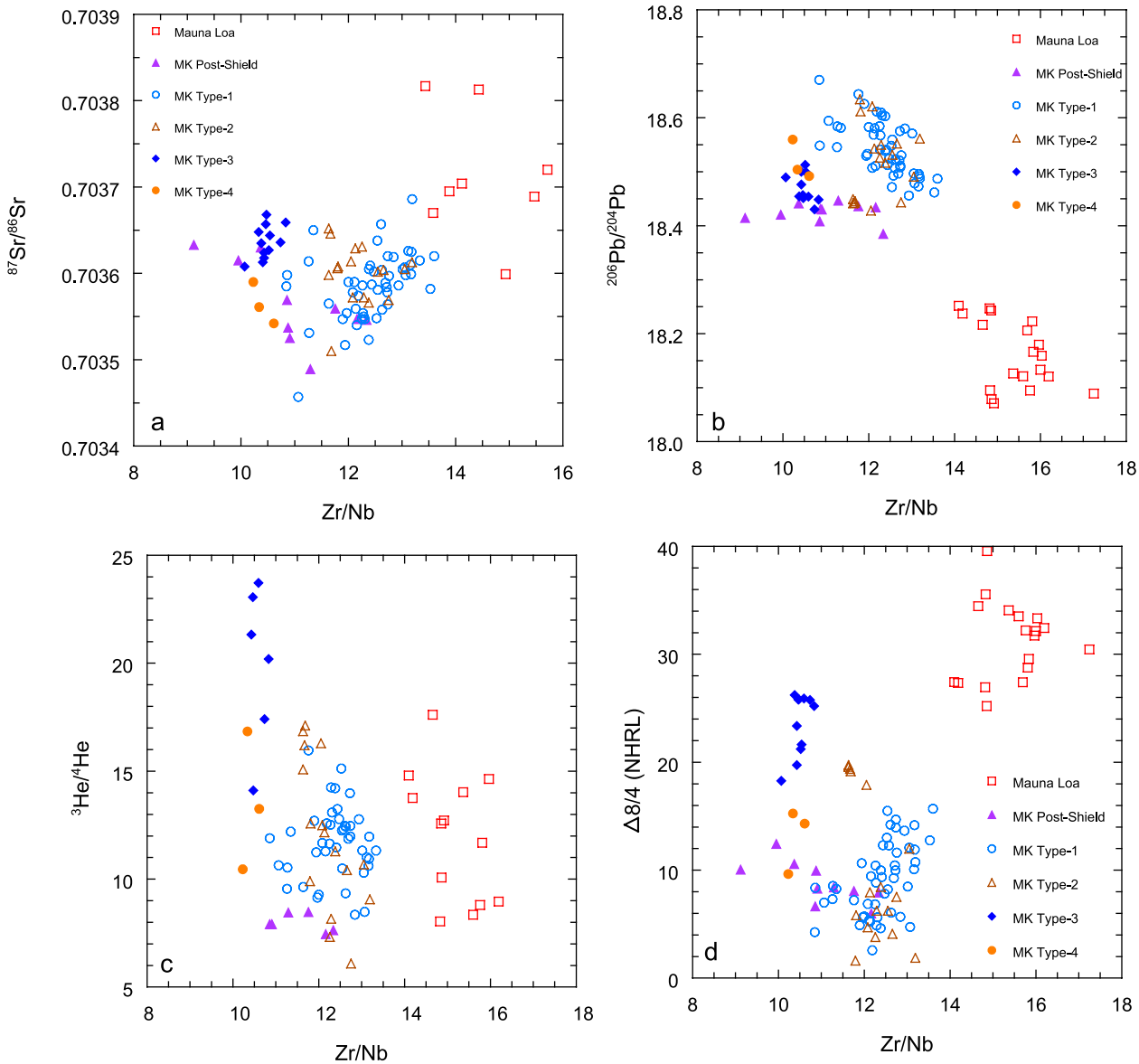

Figure 14. Zr/Nb versus isotopic ratios in HSDP-2 lavas. (a) $^{87}Sr/^{86}Sr$ data for Mauna Loa are from *Hauri et al.* [1996] and for Mauna Kea from Bryce and DePaolo (manuscript in preparation, 2003). Note the overlap in $^{87}Sr/^{86}Sr$ of deeper (older) Mauna Loa lavas with those from Mauna Kea, and the overlap in $^{87}Sr/^{86}Sr$ of the Mauna Kea magma types. (b) $^{206}Pb/^{204}Pb$ data are from *Blichert-Toft et al.* [2003]. Mauna Loa is readily distinguished from Mauna Kea in both Zr/Nb and $^{206}Pb/^{204}Pb$, but there is overlap in $^{206}Pb/^{204}Pb$ of the Mauna Kea magma types. (c) $^{3}He/^{4}He$ data are from Kurz et al. (submitted manuscript, 2003). The type-3 magmas tend toward higher $^{3}He/^{4}He$ than other Mauna Kea magmas. Mauna Loa lavas with $^{3}He/^{4}He > 12$ are from lower in the core. (d) Δ8/4 Pb values (relative to the northern hemisphere reference line [*Hart*, 1984]) versus Zr/Nb. Pb isotopic data are from *Blichert-Toft et al.* [2003]. The type-3 magmas have higher Δ8/4 Pb than other Mauna Kea magmas.

ites. Surprisingly, the type-4 lavas do not show these characteristics. In addition to the type-3 lavas, there are 5 type-2 lavas with $^{3}He/^{4}He$ and Δ8/4 values that are intermediate between those of the type-3 lavas and the rest of the main body of Mauna Kea lavas (Figure 14). Perhaps they are produced by melting a mix of the Mauna Kea and Loihi type source components?

5.2.2. Magma Production

[38] The differences in SiO_2 between the Mauna Kea lavas at a common MgO content may be

indicative of differences in the extent of melting, or the depths at which the magmas were produced and segregated in the plume. As noted above, the few melting experiments on peridotites at appropriate pressures (around 3–4 Gpa) corresponding to the proposed depths of melting in the Hawaiian plume [e.g., *Watson and McKenzie*, 1991; *Ribe and Christenson*, 1999] suggest that the composition of the magma is sensitive to the depth of magma production and segregation, and, to a lesser extent, to the extent of melting. In these experiments, the SiO_2 content of the melt decreases, and MgO content increases, with increasing pressure, whereas increased melting results in an increase in both the SiO_2 and MgO contents of the melt [*Hirose and Kushiro*, 1993; *Kushiro*, 1996; *Kogiso et al.*, 1998; *Longhi*, 2002]. On the other hand, numerous studies of associated alkalic basalts, transitional tholeiites and tholeiites have shown, in a convincing manner, that the SiO_2 content of these magmas declines with decreased melting [e.g., *Clague and Frey*, 1982; *Feigenson et al.*, 1983; *Frey et al.*, 1990; *Garcia et al.*, 1995b; *Frey et al.*, 2000].

5.2.3. Extent of Melting

[39] Despite the fact that the compositions of the postshield lavas have been compromised by alteration and shallow fractionation processes, they provide the most compelling evidence for the influence of variable amounts of melting on the SiO_2 content of the magmas. These low-SiO_2 magmas were erupted at a time of very low lava accumulation rates of around 1 mm/yr [*Sharp et al.*, 1996; DePaolo et al., manuscript in preparation, 2003], presumably a consequence of declining melt production. In these lavas, values of $SiO_2(13)$ show strong negative correlations with incompatible element ratios (Figure 15), and with incompatible element abundances normalized to 13 wt% MgO (Figure 16), indicating a decline in the SiO_2 content of the melt with decreasing melt production. For example, the increase in Sr(13), Nb(13) and Ba(13) from tholeiitic postshield lavas (e.g., unit 60) to the alkalic lava (unit 48) by a factor of around 2, is accompanied by a decrease in $SiO_2(13)$ of about 4 wt%. The implications are that doubling the amount of melt production, at these low levels of melting, increases the SiO_2 content of the melt by around 4%.

[40] When the SiO_2 data for the various tholeiitic lava types (including Mauna Loa) are normalized to a constant MgO content of 13 wt.%, using the regression equations from Table 4, there is a wide range in values of $SiO_2(13)$ values. Not unexpectedly, Mauna Loa lavas are at the high end and the type-2 and 3 Mauna Kea lavas are at the low end of the range. Plots of $SiO_2(13)$ against incompatible element ratios that decrease markedly with the extent of melting (e.g., Ba/Y, Nb/Y, Zr/Y) show broad inverse trends (Figure 15). Additionally, plots of $SiO_2(13)$ against normalized incompatible element abundances (e.g., $TiO_2(13)$, Zr(13), Nb(13)) show similar inverse trends (Figure 16). These trends support the inference that the SiO_2 content of magmas is proportional to the extent of melting, increasing from Mauna Kea postshield magmas, through Mauna Kea tholeiites, to Mauna Loa magmas. It may not, however, be as simple as that. We have argued above that the source for Mauna Loa magmas is distinct from those of Mauna Kea, and that the source of type-3 and 4 Mauna Kea magmas differs from that of the type- 1 and 2 magmas. Consequently, there is no a priori reason why the SiO_2 content and incompatible element abundances in these sources should necessarily be similar.

[41] The type-1 and 2 Mauna Kea magmas appear to be derived from a common source. By definition, they differ in $SiO_2(13)$, indicating that different processes have been at work in their production. By analogy with the postshield lavas, it seems possible that the type-2 magmas, with their lower SiO_2 contents, may have been produced by lesser amounts of melting than the type-1 magmas. The difference of 1–2% in $SiO_2(13)$ could imply that the type-2 magmas resulted from a factor of about 0.75 of the melt fraction that gave rise to the type-1 magmas. The fact that the type-2 lavas were most frequently erupted high in the stratigraphic column at a time when eruption rates were in decline [*Sharp et al.*, 1996; DePaolo et al., manuscript in preparation, 2003] adds credence to this suggestion. Table 4 and Figure 16 show that the type-2 magmas

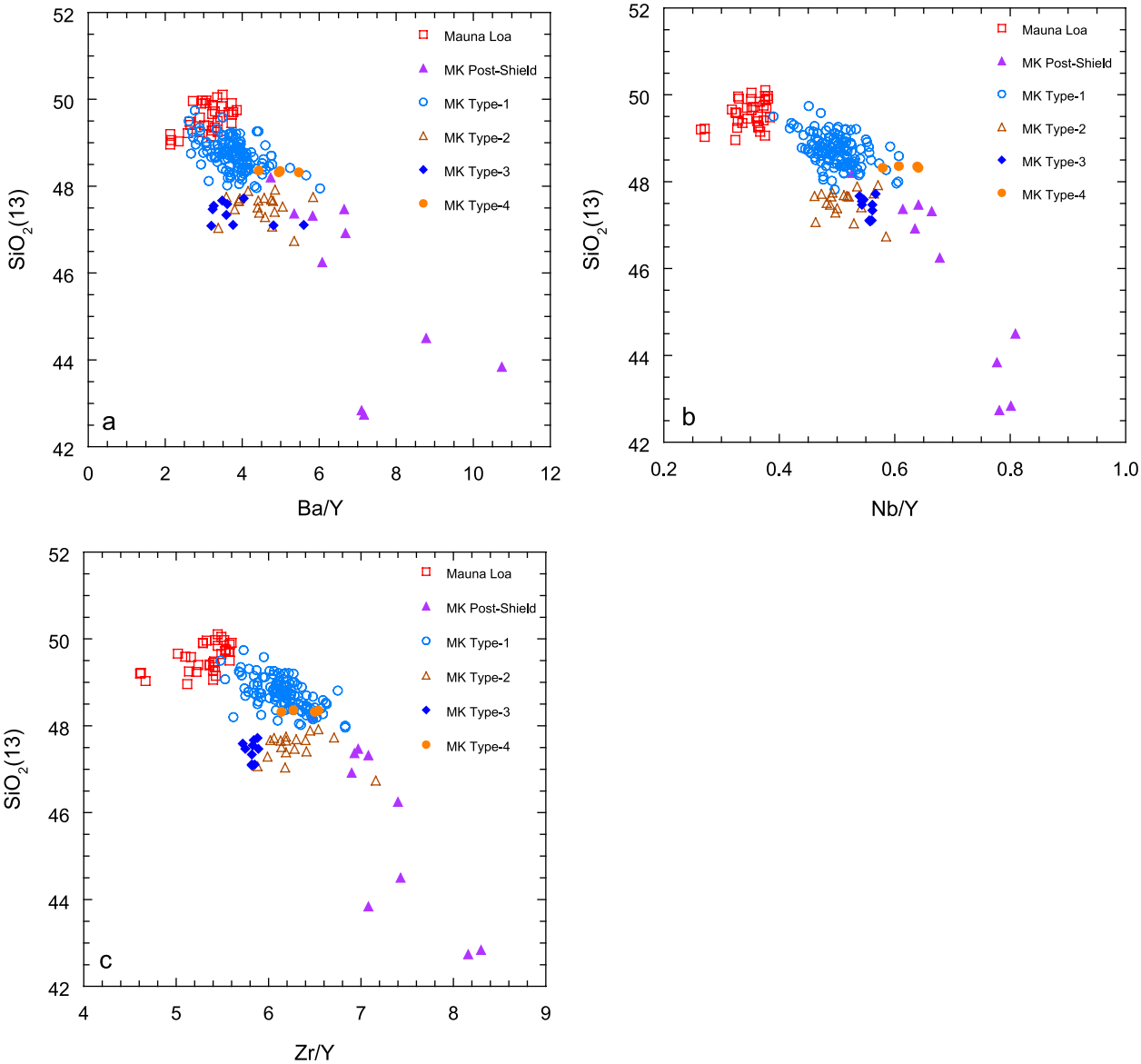

Figure 15. Variation of $SiO_2(13)$ versus incompatible element abundance ratios in HSDP-2 lavas. $SiO_2(13)$ is normalized to 13% MgO using the equations in Table 4. The data have been screened for alteration by removing samples with $K_2O/P_2O_5 < 1$.

tend, on average, to have higher normalized incompatible element abundances than the type-1 magmas. The average Ba(13) and Nb(13) of the type-2 lavas are102 and 13.2 respectively, compared with averages of 85 and 11.2 in the type-1 lavas. Incompatible element ratios also tend to be higher in the type-2 lavas (Figures 13 and 15). This could imply that the type-2 magmas were produced by a factor of around 18–20% less melt production than the type-1 magmas. There is, however, considerable overlap between the two lava types. Some type-1 lavas have ratios and normalized abundances of these elements that are just as high as any of the type 2-lavas. This would seem to imply that the extent of melting is not the major process in the generation of these two magma types. On the other hand, melting does appear to play a role in the finer details. For example, values of $SiO_2(13)$ in both type-1 and 2 lavas decrease with increasing

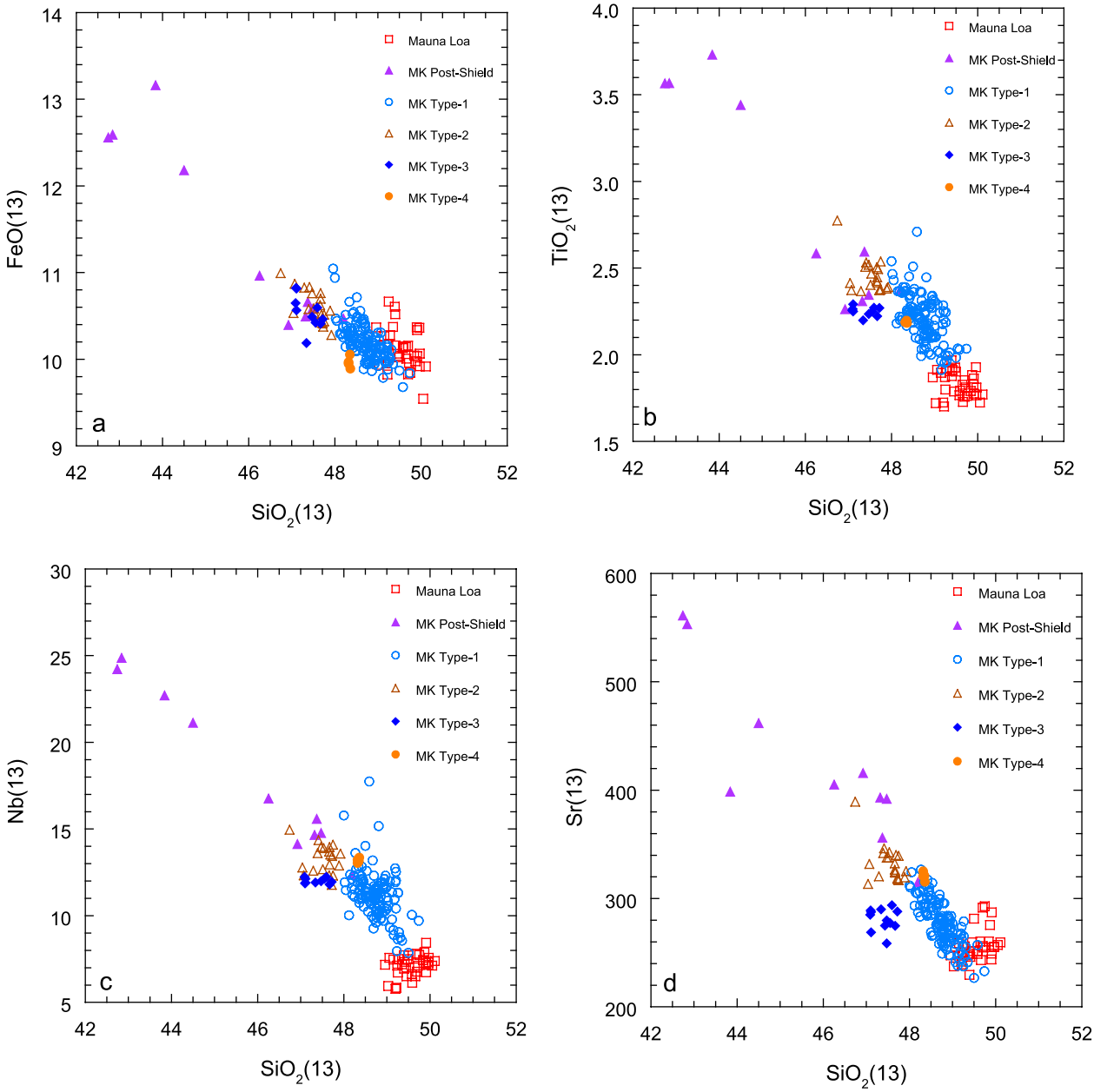

Figure 16. Normalized abundances of (a) FeO, (b) TiO_2, (c) Nb, and (d) Sr versus SiO_2 in HSDP-2 lavas. All of the data have been normalized to 13% MgO using the equations in Table 4. The data have been screened for alteration by removing samples with $K_2O/P_2O_5 < 1$.

stratigraphic height from the transition from submarine to subaerial lavas at 1070 m to 340 m at the base of the postshield lavas (Figure 10). This decrease in $SiO_2(13)$ is accompanied by corresponding increases in TiO_2/Al_2O_3, Nb/Y, Ba/Y and Zr/Y to values approaching those of the postshield lavas (Figure 1). In other words, it is indicative of a decline in melting of both magma types over time: a possible harbinger of the onset of postshield magmatism?

5.2.4. Depth of Melting and Segregation

[42] If variable amounts of melting are not responsible for the major differences in $SiO_2(13)$ between the type-1 and 2 magmas and the type-3 and 4 magmas, we are left with depth of melting and

melt segregation as the probable cause. As noted above, the available relevant melting experiments on peridotite [e.g., *Hirose and Kushiro*, 1993; *Kushiro*, 1996; *Kogiso et al.*, 1998; *Longhi*, 2002] indicate that melts produced at greater depths will have lower SiO_2 at a constant MgO than shallower melts. Conversely, the FeO content of the melt increases at a fixed MgO content with increasing pressure. The type-1 lavas have higher SiO_2(13) and lower FeO(13) than the type-2 lavas, and the type-4 have higher SiO_2(13) and lower FeO(13) than the type-3 lavas (Figure 16a). The implications are that the type-2 and 3 magmas were produced, or segregated from the peridotite residua, at greater depths in the plume than the type-1 and 4 magmas. The depth at which a melt segregates from its residua may depend on whether it is transported by porous flow along grain boundaries or migrates into interconnecting channels [e.g., *Mckenzie*, 1985; *Ribe*, 1988; *Spiegelman and Kenyon*, 1992]. Melt percolation is more likely to result in segregation at shallower levels in the plume than channelized flow. This scenario may explain why picrites predominate in the type-2 and 3 lavas, and why there are fewer low-MgO lavas than among types 1 and 4 lavas. Melt percolation is likely to result in melt and wall rock-reaction [*Kelemen et al.*, 1992], resulting in a change in magma composition from picrite toward a more basaltic composition. Mixing of this magma with the low-MgO "steady state" magma in the shallow magma reservoir is less likely to pull the overall composition far into the olivine field, resulting in a spectrum of compositions ranging from low-MgO basalts to picrites. On the other hand, melts that migrate in channels are less likely to react with the wall rock, resulting in the delivery of picrites to the magma reservoir. Mixing of these picrites with the low-MgO "steady state" magma will result in overall compositions with high MgO contents, and may well disguise the fact that low-MgO magmas were involved at all.

5.2.5. Magmatic Evolution

[43] In this section we will utilize lava accumulation rate models [*DePaolo and Stolper*, 1996; DePaolo et al., manuscript in preparation, 2003; Sharp et al., submitted manuscript, 2003] to place the magmatic evolution of Mauna Kea in a tentative time frame. According to these models, the 2815 m of Mauna Kea core represent a 400 ka eruptive record, from the oldest submarine lavas at around 550 ka to the youngest subaerial postshield lavas of about 150 ka. During this time, Mauna Kea will have traversed about 40 km of the Hawaiian plume (assuming a 9–10 cm/yr northeasterly movement of the Pacific plate). Subsequent dating will probably necessitate a revision of this time frame, but relative relationships should remain intact.

[44] At around 550 ka, magma supply rates are inferred to be high, about 18 mm/yr (DePaolo et al., manuscript in preparation, 2003), with two distinct magmas, types-1 and 3, supplying the volcano. The type-3 lavas are inter-layered with type-1 lavas, tending to form packages of pillow lavas, hyaloclastites and massive units. They are particularly abundant between 1974 to 2600 m, roughly around 490–530 ka. It may be that these packages were erupted rapidly. The two magma types require different plume source components, implying that, at this time, the plume was heterogeneous at the scale of melting. The source of the type-3 magmas has lower Zr/Nb and higher $^{3}He/^{4}He$ and $^{208}Pb/^{204}Pb$ relative to $^{206}Pb/^{204}Pb$ and therefore contains higher proportions of the proposed Loihi component than the source of the type-1 magmas, which is close to the Kilauea endmember of the Hawaiian tholeiitic array. The low SiO_2(13) content of the type-3 magmas, also characteristic of Loihi tholeiites, may be inherited from the source, but it could also be a consequence of melt segregation from its residua at greater depth in the plume. This latter suggestion is supported to some extent by the presence of rare type-4 lavas in the core. These are chemically similar to the type-3 lavas, except that they have higher SiO_2(13), and may, therefore, have segregated at shallower levels in the plume. The problems with this interpretation are that the small number of samples (3) of type-4 lavas do not have the high $^{3}He/^{4}He$ and $^{208}Pb/^{204}Pb$ of the type-3 lavas.

[45] What is the origin of the type-3 magma? Is it intrinsic to Mauna Kea, representing an early stage in the volcano's development, or were these lavas

erupted on another adjacent volcano? *Holcomb et al.* [2000] propose that a southeast rift zone of Kohala extends below Mauna Kea, predicting that Kohala lavas will be encountered at depth in the drill hole. Could the type-3 magmas be lavas from Kohala volcano, erupted from such a putative southeast rift zone? They do not resemble any Kohala lava analyzed to date [*Feigenson et al.*, 1984; *Rhodes and Weis*, 2001], but there is no a priori reason why they should. If the low SiO_2 lavas are derived from Kohala volcano, then according to the Holcomb et al. model one might expect them to lie at the base of the stratigraphic section, rather than inter-layered with more normal, type-1, Mauna Kea lavas over an interval that may well reflect more than 50 ka of eruptive history. At the time in question, around 495 to 550 ka, Kohala should have been in a vigorous stage of tholeiitic shield-building. [*Moore and Clague*, 1992]. The type-3 magmas resemble Loihi tholeiites, that is, magmas produced during the early stages of submarine shield building. If this is the case, and the type-3 magmas represent this early submarine stage of Mauna Kea, then further drilling should encounter fewer type-1 lavas and more of type-3, perhaps inter-layered with alkalic lavas, as are currently found on Loihi [*Garcia et al.*, 1993, 1995b].

[46] Above 1974 m there are no more type-3 lavas in the core. In other words, the source of these magmas has been exhausted from Mauna Kea's melting zone after about 495 ka. Throughout the rest of the stratigraphic section until the onset of postshield magmatism at around 280 ka, that is, for over 200 ka, the eruptive sequence consists of inter-layered type-1 and 2 lavas. These are derived from a common Mauna Kea source, with only minor fluctuations in isotopic ratios [Bryce and DePaolo, manuscript in preparation, 2003; *Blichert-Toft et al.*, 2003] attesting to small variations in the source components. The principal difference between these two magma types is in the depth at which they melted, or segregated from their source residua. Type-2 lavas are relatively infrequent below the submarine to subaerial transition at 1080 m (about 440 ka), but become increasingly abundant above 850 m, suggesting that deep melt segregation became more common after around 400 ka.

[47] At around 440 ka, there appears to have been a fundamental transition in the magmatic plumbing system of Mauna Kea. Four things happened simultaneously: (1) the inferred lava accumulation rate dropped from around 15 mm/yr to around 5 mm/yr, subsequently declining to below 3 mm/yr (DePaolo et al., manuscript in preparation, 2003); (2) low-MgO lavas (7–9% MgO) became much more prevalent, especially in the type-1 lavas; (3) the SiO_2(13) of both type-1 and type-2 magmas began to decline; (4) incompatible element ratios (e.g., TiO_2/Al_2O_3, Ba/Y, Nb/Y, Zr/Y) in type-1 and 2 magmas began to increase. All of these factors point to a dwindling magma supply, leading up to the onset of postshield volcanism as the volcano moves toward the margin of the plume. Note, however, that there is no accompanying change in source components.

[48] With the onset of postshield volcanism at 337 m, inferred to be at around 270 ka, the data become scattered, ranging from tholeiites to alkalic basalts. There are no coherent trends, and many of the lavas have evolved beyond olivine-control. All of this is consistent with low lava accumulation rates (1–2 mm/yr) as a consequence of low magma supply, resulting in ephemeral magma reservoirs [*Frey et al.*, 1990].

5.3. Origin and Evolution of Mauna Loa Magmas

[49] Throughout the 245 m of Mauna Loa core, the trends for major elements and compatible trace elements have remained remarkably coherent, and indistinguishable from those of modern historical lavas. Although incompatible element abundances and ratios tend, on average, to be lower than in historical lavas, they are within, or just below, the overall range of historical lavas. In many respects they are similar to the lavas erupted around 1880–1887, when eruption rates were high [*Rhodes and Hart*, 1995]. There are, however, some differences. First, picrites (MgO > 12%) are much more abundant in the HSDP-2 core than in the historical record, or among young (<36 ka) prehistoric lavas. Picrites constitute about 61% of the samples in the

core, but only 7% of the historical record and 14% of <36 ka prehistoric lavas. There are two possible explanations: either Mauna Loa magmas were hotter and therefore more picritic in the past, or hot, mobile picritic magmas are more likely to travel the 30–40 km from Mauna Loa's northeast rift zone to the drill site than cooler tholeiitic magmas [*Rhodes*, 1996]. For reasons given below, we suspect that the latter explanation is the more probable.

5.3.1. Magma Source

[50] Trace element ratios involving Nb that are sensitive to changes in source components are relatively constant in the Mauna Loa lavas. Most of the variation in Zr/Nb and Nb/Y can be attributed to differences in the degree of melting (Figure 13), or slight variations in the proportions of source components [*Rhodes and Hart*, 1995]. There are no apparent systematic change in these ratios with depth in the core. On the other hand, there are subtle changes in isotopic ratios with depth. For example, $^{3}He/^{4}He$ is higher than 12 below 214 m in the pilot hole [*DePaolo et al.*, 2001] and 163 m in the present hole (Kurz et al., submitted manuscript, 2003), and $^{208}Pb/^{204}Pb$ increases slightly with increasing depth in both the pilot hole [*DePaolo et al.*, 2000] and this hole [*Blichert-Toft et al.*, 2003]. Additionally, $^{87}Sr/^{86}Sr$ data from the pilot hole [*Hauri et al.*, 1996] is less than 0.7037 below 241 m. These changes are consistent with an increase in Kilauea or Loihi components with age in the source of Mauna Loa magmas, toward source compositions that are intermediate between those of modern Mauna Loa and Kilauea. In this respect, the source of the oldest Mauna Loa lavas sampled by the drill core is approaching that of >100 ka lavas from the submarine section of Mauna Loa's southwest rift zone [*Kurz et al.*, 1995; Rhodes et al., manuscript in preparation, 2003].

5.3.2. Magma Production

[51] The variation in SiO_2 with MgO is very coherent (Figure 5), especially after screening for possible alteration effects and loss of SiO_2 by removing samples with $K_2O/P_2O_5 < 1$. Consequently, the average value of SiO_2, when normalized to 13% MgO ($SiO_2(13)$) using the equation in Table 4, is remarkably constant at 49.6 ± 0.3. Normalized values for other major elements are also very uniform. We interpret this constancy, together with the similarity of SiO_2 and other major element trends with historical lavas, as evidence that the processes of melting and the depth of melt segregation for Mauna Loa, unlike Mauna Kea, have remained remarkably uniform. The extent of melting, however, and hence magma supply, may have been more variable. We know from historical lavas that incompatible element ratios are low when eruption rates are high [*Rhodes and Hart*, 1995]. The small increase in incompatible element ratios with stratigraphic height may, therefore, indicate a decrease in melting and eruption rates with time. Support for this suggestion comes from the corresponding gradual decrease in the MgO content of the low MgO lavas, implying that magma supply rates were higher in the past, thus pulling the composition of the quasi steady state magma further into the olivine stability field. This suggests that for lavas near the bottom of the Mauna Loa section of the core, eruption rates were higher than the highest historical rates of 0.05 km^3/yr [*Lockwood and Lipman*, 1987], and probably approaching those of modern Kilauea (about 0.06–1.0 km^3/yr) [*Dzurisin et al.*, 1984; *Cayol et al.*, 2000].

5.3.3. Magmatic Evolution

[52] The pilot hole of the Hawaii Scientific Drilling Project sampled 280 m of Mauna Loa lavas ranging in age from about 1.3 ka (the Panaewa picrite) to around 100 ka [*Sharp et al.*, 1996; J. M. Rhodes, H. Guillou, F. A. Trusdell, and M. O. Garcia, Is Mauna Loa Volcano in Decline?, *Bulletin of Volcanology*, 2003]. Although there is, as yet, no comparable age information for the Mauna Loa section of the current drill core, we assume that the age range is about the same, that is, around 100 ka. Over this time, Mauna Loa will have traversed and sampled about 10 km across the Hawaiian plume (assuming a 9–10 cm/yr northeasterly movement of the Pacific plate).

[53] The high value and constancy of $SiO_2(13)$ together with the constancy of other major element data suggest that melt segregation was relatively

shallow, and that melting processes and depth of melt segregation have not changed significantly over the last 100 ka. Furthermore, the presence of low-MgO quasi steady state magmas together with picrites may indicate that melt extraction was dominated by porous flow rather than channelized flow. These conclusions are consistent with those of Rhodes et al. (manuscript in preparation, 2003) for even older lavas (>100 ka) from Mauna Loa's submarine southwest rift zone. We have presented evidence above that during this 100 ka, although melting processes and the depth of melt segregation have remained relatively constant, there has been a small shift in the preponderance of source components toward a greater proportion of the Kilauea or Loihi components. This trend is continued further in >100 ka lavas sampled from a submarine landslide scarp on Mauna Loa's southwest rift zone [*Kurz et al.*, 1995; Rhodes et al., manuscript in preparation, 2003]. Over this same time interval there appears also to have also been a small decline in melt production. The timing of these changes is critical, but difficult to establish because of inadequate age information. Data for ^{14}C dated flows [*Lockwood*, 1995] going back about 30–36 ka indicate that the change in source components, and possible decline in melt production, occurred before then. On the other hand, extrapolating age information from the pilot hole [*Lipman and Moore*, 1996] suggests that the decline in $^{3}He/^{4}He$ and increase in $^{87}Sr/^{86}Sr$ may have occurred around 60–80 ka. In summary, there have been subtle changes in source components, and perhaps a slight decline in melt production during the last 100 ka: all consistent with the notion that Mauna Loa is moving away from the plume axis.

[54] *Lipman* [1995] suggests Mauna Loa is in decline and is approaching the postshield stage. This suggestion gains some credence from the inferred reduction in melt production, and from the reduction in $^{3}He/^{4}He$, discussed above. Events on Mauna Kea may, perhaps, be taken as a guide to what will happen on Mauna Loa. For example, the decrease in $^{3}He/^{4}He$ (Kurz et al., submitted manuscript, 2003) to values comparable to those on Mauna Loa after 60–80 ka, occurred at a depth of 670 m, corresponding to a model age of around 377 ka (DePaolo et al., manuscript in preparation, 2003), almost 100 ka before the advent of postshield volcanism. This could be taken to indicate that we might expect the onset of postshield volcanism on Mauna Loa in another 20–40 ka. On the other hand, postshield volcanism on Mauna Kea was preceded by a 140 ka period in which declining eruption rates were accompanied by decreasing $SiO_2(13)$ in both type-1 and type-2 lavas (Figure 10), presumably a consequence of decreasing melt production as Mauna Kea moved toward the periphery of the plume. There is no indication of a similar decline in $SiO_2(13)$ in the Mauna Loa record, implying that postshield volcanism may be a long time coming. Perhaps the announcement of Mauna Loa's demise (to paraphrase Mark Twain) is greatly exaggerated!

6. Conclusions

[55] 1. The Hawaii Scientific Drilling Project sampled 3098 m of basaltic lavas from Mauna Loa and Mauna Kea volcanoes. The transition from Mauna Loa to Mauna Kea lavas at 245 m is recognized using geochemical discriminants. The geochemical record is inferred to reflect about 100 ka and 400 ka of the magmatic history of Mauna Loa and Mauna Kea respectively, as they transit the Hawaiian plume.

[56] 2. The Mauna Loa lavas are chemically distinct from Mauna Kea lavas. The Mauna Kea lavas are subdivided into a thin upper 107 m sequence of postshield tholeiites, transitional tholeiites and alkali basalts contemporaneous with the Hamakua Volcanics, and four tholeiitic lava types that occur throughout the rest of the core. These four lava types are recognized on the basis of MgO-normalized SiO_2 and Zr/Nb ratios. Type-1 lavas (high SiO_2 and Zr/Nb) are ubiquitous below the postshield lavas and are the dominant magma type on Mauna Kea, inter-layered with the other three lava types. Type-2 lavas (low SiO_2 but high Zr/Nb) are found only in the upper core, and especially above 850 m. Type-3 lavas (low SiO_2 and Zr/Nb) are remarkably similar to tholeiites from Loihi volcano and are present only below 1974 m. There are only 3

flows of type-4 lavas (high SiO_2 and low Zr/Nb). They are present in the upper and lower core.

[57] 3. All of the tholeiites show strong, coherent, linear major and trace element trends with MgO. These trends are not simply a consequence of accumulation and fractionation of olivine as is commonly supposed. Mixing between picritic magmas (13–15% MgO), accumulated or entrained olivine phenocrysts and xenocrysts, and consanguineous low-MgO (7–8% MgO) "steady state" magmas is required to explain the linear trends.

[58] 4. A fundamental change occurred in Mauna Kea's magmatic plumbing system at around 440 ka. The onset of these changes corresponds with a gradual decline in melt production and decreasing eruption rates, foreshadowing the onset of postshield volcanism.

[59] 5. The postshield lavas, erupted between 337 and 246 m, have compositions indicative of low but varying melt production, an inference supported by very low eruption rates. As a consequence many postshield lavas, unlike earlier lavas, show evidence of extensive fractionation, beyond olivine control. An additional consequence of the low magma supply and eruption rates is that postshield lavas are more altered than other lavas.

[60] 6. The drill core is inferred to have sampled about 400 ka of Mauna Kea's magmatic history, from about 550 to 150 ka. During this period, Mauna Kea will have traversed about 40 km of the Hawaiian plume. At the start of this record, eruption rates were high and two distinct tholeiitic magmas (type-1 and -3) were erupting concurrently. These two magmas require two distinct source components, one similar to that of Loihi tholeiites and the other close to that of Kilauea magmas. At around 495 ka the Loihi-like source of the type-3 magmas was exhausted, and these lavas are absent from the rest of the core. For the next 200 ka or so, the eruptive sequence consists of inter-layered type-1 and -2 lavas that are derived from a common Mauna Kea source, the major difference between the two being the depth at which the melts segregated from the source. Around 440 ka, which corresponds with the submarine to subaerial transition in the drill core, melting and eruption rates began to decline gradually, until at 280 ka they were so low as to initiate the onset of about 130 ka of postshield magmatism.

[61] 7. The trends for major elements and compatible trace elements in Mauna Loa tholeites are remarkably coherent throughout the core, and indistinguishable from those of modern historical lavas. In particular, MgO-normalized SiO_2 values have remained constant. We interpret this to indicate that the depth of melt segregation has remained uniform and shallow over the last 100 ka. There are, however, small decreases in incompatible element abundances and ratios with depth, perhaps indicating that melting, and therefore magma supply, was slightly higher in the past than it is today. Similarly, there have been small shifts in the isotopic ratios of Sr, Pb and He, indicating that there may once have been slightly more of a Kilauea or Loihi component in the source than at present. We speculate that this change possibly occurred around 60–80 ka ago, but that, nonetheless, Mauna Loa is a long way away from its eventual transition to postshield volcanism.

Acknowledgments

[62] Special thanks to D. DePaolo, E. Stolper and D. Thomas for their leadership of the Hawaii Scientific Drilling Project. Also to M. Garcia, C. Seaman and the crew at the rig site for a superb job of core-handling and documentation, and to our colleagues in the project for their unselfish sharing of data. The paper benefited from thoughtful reviews by C. Rhodes, T. Cobleigh and an anonymous reviewer. The exhaustive comments of Dave Clague, although exhausting, were very much appreciated and improved the content of the paper. The XRF lab at Umass was, as always, ably maintained by P. Dawson. This research was supported by the Geodynamics Program of the National Science Foundation.

References

Baker, M. B., S. Alves, and E. M. Stolper (1996), Petrography and petrology of the Hawaiian Scientific Project lavas: Inferences from olivine phenocryst abundances and compositions, *J. Geophys. Res.*, *101*, 11,715–11,727.

Basaltic Volcanism Study Project (1981), *Basaltic Volcanism on the Terrestrial Planets*, Pergamon Press, New York.

Blichert-Toft, J., D. Weis, C. Maerschalk, A. Agranier, and F. Albarède (2003), Hawaiian hot spot dynamics as inferred from the Hf and Pb isotope evolution of Mauna Kea volcano, *Geochem. Geophys. Geosyst.*, *4*(2), 8704, doi:10.1029/2002GC000340.

Budahn, J. R., and R. A. Schmitt (1985), Petrogenetic modeling of Hawaiian tholeiitic basalts: A geochemical approach, *Geochim. Cosmochim. Acta*, *49*, 67–87.

Carmichael, I. S. E., F. J. Turner, and F. Verhoogen (1974), *Igneous Petrology*, McGraw-Hill, New York.

Cayol, V., J. H. Dietrich, A. T. Okamura, and A. Miklius (2000), High magma storeage rates before the 1983 eruption of Kilauea, Hawaii, *Science*, *288*, 2343–2346.

Chen, C.-Y., F. A. Frey, J. M. Rhodes, and R. M. Easton (1996), Temporal geochemical evolution of Kilauea Volcano: Comparison of Hilina and Puna basalt, in *Earth Processes: Reading the Isotopic*, *Geophys. Monogr. Ser.*, vol. 95, edited by A. Basu and S. R. Hart, pp. 161–181, AGU, Washington, D. C.

Clague, D. A., and G. B. Dalrymple (1987), The Hawaiian—Emperor volcanic chain: Part I. Geologic evolution, *U.S. Geol. Surv. Prof. Paper*, *1350*, 5–54.

Clague, D. A., and F. A. Frey (1982), Petrology and trace element geochemistry of the Honolulu Volcanics, Ohahu: Implications for the oceanic mantle below Hawaii, *J. Petrol.*, *23*, 447–504.

Clague, D. A., W. S. Weber, and J. E. Dixon (1991), Picritic glasses from Hawaii, *Nature*, *353*, 553–556.

Clague, D. A., J. G. Moore, J. E. Dixon, and W. B. Friesen (1995), Petrology of submarine lavas from Kilauea's Puna Ridge, Hawaii, *J. Petrol.*, *36*, 299–349.

Defant, M. J., and R. L. Nielsen (1990), Interpretation of open system petrogenetic processes: Phase equilibria constraints on magma evolution, *Geochim. Cosmochim. Acta*, *54*, 87–102.

DePaolo, D. J., and E. M. Stolper (1996), Models of Hawaiian volcano growth and plume structure: Implications of results from the Hawaii Scientific Drilling Project, *J. Geophys. Res.*, *101*, 11,643–11,654.

DePaolo, D. J., J. G. Bryce, A. Dodson, D. L. Shuster, and B. MackKennedy (2001), Isotopic evolution of Mauna Loa and the chemical structure of the Hawaiian plume, *Geochem. Geophys. Geosyst.*, *2*, Paper number 2000GC000139.

Dzurisin, D., R. Y. Koyanagi, and T. T. English (1984), Magma supply and storage at Kilauea volcano, Hawaii, 1956–1983, *J. Volcanol. Geotherm. Res.*, *21*, 177–206.

Eiler, J. M., K. A. Farley, and E. M. Stolper (1998), Correlated helium and lead isotope variations in Hawaiian lavas, *Geochim. Cosmochim. Acta*, *62*, 1977–1984.

Feigenson, M. D., A. W. Hofmann, and F. J. Spera (1983), Case studies on the origin of basalt: II. The transition from tholeiitic to alkalic volcanism on Kohala volcano, Hawaii, *Contrib. Mineral. Petrol.*, *84*, 390–405.

Frey, F. A., and J. M. Rhodes (1993), Inter-shield geochemical differences among Hawaiian volcanoes: Implications for source compositions, melting processes and magma ascent paths, *Philos. Trans. R. Soc. London Part A*, *342*, 121–136.

Frey, F. A., M. O. Garcia, W. S. Wise, A. Kennedy, P. Gurrriet, and F. Albarede (1990), Evolution of Mauna Kea volcano, Hawaii: Petrologic and geochemical constraints on post-shield volcanism, *J. Geophys. Res.*, *95*, 1271–1300.

Frey, F. A., W. S. Wise, M. O. Garcia, H. West, S.-T. Kwon, and A. Kennedy (1991), Evolution of Mauna Kea volcano, Hawaii: Petrogenesis of tholeiitic and alkalic basalts, *J. Geophys. Res.*, *96*, 14,347–14,375.

Frey, F. A., M. O. Garcia, and M. F. Roden (1994), Geochemical characteristics of Koolau volcano: Implications of intershield geochemical differences among Hawaiian volcanoes, *Geochim. Cosmochim. Acta*, *58*, 1441–1462.

Frey, F. A., D. Clague, J. J. Mahoney, and J. M. Sinton (2000), Volcanism at the edge of the Hawaiian plume: Petrogenesis of submarine alkalic lavas from the North Arch volcanic field, *J. Petrol.*, *41*, 667–691.

Garcia, M. O. (1996), Petrography and olivine and glass chemistry of lavas from the Hawaii Scientific Drilling Project, *J. Geophys. Res.*, *101*, 11,701–11,713.

Garcia, M. O., B. Jorgenson, J. J. Mahoney, E. Ito, and A. J. Irving (1993), An evaluation of temporal geochemical evolution of Loihi seamount lavas: Results from Alvin submersible dives, *J. Geophys. Res.*, *98*, 357–380.

Garcia, M. O., T. P. Hulsebosch, and J. M. Rhodes (1995a), Olivine-rich submarine basalts from the southwest rift zone of Mauna Loa volcano: Implications for magmatic processes and geochemical evolution, in *Mauna Loa Revealed: Structure, Composition, History and Hazards*, *Geophys. Monogr. Ser.*, vol. 92, edited by J. M. Rhodes and J. P. Lockwood, pp. 45–80, AGU, Washington, D. C.

Garcia, M. O., D. J. P. Foss, H. B. West, and J. J. Mahoney (1995b), Geochemical and isotopic evolution of Loihi volcano, Hawaii, *J. Petrol.*, *36*, 1647–1674.

Garcia, M. O., A. J. Pietruszka, and J. M. Rhodes (2004), A petrologic perspective of the summit magma chamber of Kilauea Volcano, *J. Petrol.*, in press.

Griffith, R. W., and I. H. Cambell (1990), Stirring and structure in mantle starting plume, *Earth Planet. Sci. Lett.*, *99*, 66–78.

Hart, S. R. (1984), A large-scale isotope anomaly in the southern hemisphere mantle, *Nature*, *309*, 753–757.

Hart, S. A., and K. E. Davis (1978), Nickel partitioning between olivine and silicate melt, *Earth Planet. Sci. Lett.*, *40*, 203–219.

Hauri, E. H. (1996), Major-element variability in the Hawaiian mantle plume, *Nature*, *382*, 415–419.

Hauri, E. H., J. A. Whitehead, and S. R. Hart (1994), Fluid dynamic and geochemical aspects of entrainment in mantle plumes, *J. Geophys. Res.*, *99*, 24,275–24,300.

Hauri, E. H., J. C. Lassiter, and D. J. DePaolo (1996), Osmium isotope systematics of drilled lavas from Mauna Loa, Hawaii, *J. Geophys. Res.*, *101*, 11,793–11,806.

Helz, R. T., and C. R. Thornber (1987), Geothermometry of of Kilauea Iki lava lake, Hawaii, *Bull. Volcanol.*, *49*, 651–658.

Hirose, K., and I. Kushiro (1993), Partial melting of dry peridotites at high pressure: Determination of composition of melts segregated from peridotite using aggregates of diamonds, *Earth Planet. Sci. Lett.*, *114*, 477–489.

Holcomb, R. T., B. K. Nelson, P. W. Reiners, and N.-L. Sawyer (2000), Overlapping volcanoes: The origin of Hilo Ridge, Hawaii, *Geology*, *28*, 547–550.

Huang, S., and F. A. Frey (2003), Trace element abundances of Mauna Kea basalt from phase 2 of the Hawaii Scientific Drilling Project: Petrogenetic implications of correlations

with major element content and isotopic ratios, *Geochem. Geophys. Geosyst.*, *4*(6), 8711, doi:10.1029/2002GC000322.

Kelemen, P. B., H. J. B. Dick, and J. E. Quick (1992), Formation of harzburgite by pervasive melt/rock reaction in the upper mantle, *Nature*, *358*, 635–641.

Kinzler, R. J., T. L. Grove, and S. I. Recca (1990), An experimental study on the effect of temperature and melt composition on the partitioning of nickel between olivine and silicate melt, *Geochim. Cosmochim. Acta*, *54*, 1255–1265.

Kogiso, T., K. Hirose, and E. Takahashi (1998), Melting experiments on homogeneous mixtures of peridotite and basalt: Application to the genesis of ocean island basalts, *Earth Planet. Sci. Lett.*, *162*, 45–61.

Kurz, M. D., T. C. Kenna, D. P. Kammer, and J. M. Rhodes (1995), Isotopic evolution of Mauna Loa volcano: A view from the submarine southwest rift zone, in *Mauna Loa Revealed: Structure, Composition, History and Hazards*, *Geophys. Monogr. Ser.*, vol. 92, edited by J. M. Rhodes and J. P. Lockwood, pp. 45–80, AGU, Washington, D. C.

Kushiro, I. (1996), Partial melting of fertile mantle peridotite at high pressures: An experimental study using aggregates of diamond, in *Earth Processes: Reading the Isotopic*, *Geophys. Monogr. Ser.*, vol. 95, edited by A. Basu and S. R. Hart, pp. 109–122, AGU, Washington, D. C.

Lassiter, J. C., and E. H. Hauri (1998), Osmium isotope variations in Hawaiian lavas: Evidence for recycled lithosphere in the Hawaiian plume, *Earth Planet. Sci. Lett.*, *164*, 483–496.

Lassiter, J. C., D. J. DePaolo, and M. Tatsumoto (1996), Isotopic evolution of Mauna Kea volcano: Results from the initial phase of the Hawaii Scientific Drilling Project, *J. Geophys. Res.*, *101*, 11,769–11,780.

Le Bas, M. J. (2000), IUGS reclassification of the high-Mg and picritic volcanic rocks, *J. Petrol.*, *41*, 1467–1470.

Lipman, P. W. (1995), Declining growth rate of Mauna Loa during the last 10,0000 years: Rates of lava accumulation versus gravitational subsidence, in *Mauna Loa Revealed: Structure, Composition, History and Hazards*, *Geophys. Monogr. Ser.*, vol. 92, edited by J. M. Rhodes and J. P. Lockwood, pp. 45–80, AGU, Washington, D. C.

Lipman, P. W., and J. G. Moore (1996), Mauna Loa lava accumulation rates at the Hilo drill site: Formation of lava deltas during a period of declining overall volcanic growth, *J. Geophys. Res.*, *101*, 11,631–11,641.

Lipman, P. W., J. M. Rhodes, and G. B. Dalrymple (1990), The Ninole basalt: Implications for the structural evolution of Mauna Loa volcano, Hawaii, *Bull. Volcan.*, *53*, 1–19.

Lockwood, J. P. (1995), Mauna Loa eruptive history: The preliminary radiocarbon record, in *Mauna Loa Revealed: Structure, Composition, History and Hazards*, *Geophys. Monogr. Ser.*, vol. 92, edited by J. M. Rhodes and J. P. Lockwood, pp. 45–80, AGU, Washington, D. C.

Lockwood, J. P., and P. W. Lipman (1987), Holocene eruptive history of Mauna Loa volcano, *U.S. Geol. Surv. Prof. Pap.*, *1350*, 509–535.

Longhi, J. (2002), Some phase equilibria systematics of lherzolite melting: I, *Geochem. Geophys. Geosyst.*, *2*, Paper number 2001GC000204.

Maaløe, S. (1979), Compositional range of primary tholeiitic magmas evaluated from major-element trends, *Lithos*, *12*, 59–72.

Macdonald, G. A. (1963), Relative abundance of intermediate members of the oceanic basalts: A discussion, *J. Geophys. Res.*, *68*, 5100–5102.

Macdonald, G. A. (1968), Composition and origin of Hawaiian lavas, *Mem. Geol. Soc. Am.*, *116*, 477–522.

Maxwell, J. A. (1968), *Rock and Mineral Analysis*, pp. 419–421, Interscience, New York.

McKenzie, D. (1985), The extraction of magma from the crust and mantle, *Earth Planet. Sci. Lett.*, *74*, 149–157.

Montierth, C., A. D. Johnston, and K. V. Cashman (1995), An empirical glass-composition-based geothermometer for Mauna Loa lavas, in *Mauna Loa Revealed: Structure, Composition, History and Hazards*, *Geophys. Monogr. Ser.*, vol. 92, edited by J. M. Rhodes and J. P. Lockwood, pp. 207–217, AGU, Washington, D. C.

Moore, J. G., and D. A. Clague (1992), Volcano growth and the evolution of Hawaii, *Bull. Geol. Soc. Am.*, *104*, 1471–1484.

Murata, K. J., and D. H. Richter (1966), Chemistry of lavas of the 1959–60 eruption of Kilauea volcano, Hawaii, *U.S. Geol. Surv. Prof. Pap.*, *537-A*, 26 pp.

Norman, M. D., and M. O. Garcia (1999), Primitive magmas and source characteristics of the Hawaiian plume: Petrology and geochemistry of shield picrites, *Earth Planet. Sci. Lett.*, *168*, 27–44.

O'Hara, M. J. (1977), Geochemical evolution during fractional crystallization of a periodically refilled magma chamber, *Nature*, *266*, 503–507.

Powers, H. A. (1955), Composition and origin of basaltic magmas on the Hawaiian islands, *Geochim. Cosmochim. Acta*, *7*, 77–107.

Quane, S. L., M. O. Garcia, H. Guillou, and T. P. Hulsebosch (2000), Magmatic history of the east rift zone of Kilauea volcano, Hawaii based on drill core from SOH 1, *J. Volcanol. Geotherm. Res.*, *102*, 319–338.

Rhodes, J. M. (1988), Geochemistry of the 1984 Mauna Loa eruption: Implications for magma storage and supply, *J. Geophys. Res.*, *93*, 4453–4466.

Rhodes, J. M. (1995), The 1852 and 1868 Mauna Loa picrite eruptions: Clues to parental magma compositions and the magmatic plumbing system, in *Mauna Loa Revealed: Structure, Composition, History and Hazards*, *Geophys. Monogr. Ser.*, vol. 92, edited by J. M. Rhodes and J. P. Lockwood, pp. 241–262, AGU, Washington, D. C.

Rhodes, J. M. (1996), Geochemical stratigraphy of lava flows sampled by the Hawaii Scientific Drilling Project, *J. Geophys. Res.*, *101*, 11,729–11,746.

Rhodes, J. M. (2000), Geochemistry of Mauna Loa and Mauna Kea lavas sampled by the Hawaii Scientific Drilling Project, *Eos Trans. AGU*, *81*(48), Fall Meet. Suppl., F1342.

Rhodes, J. M., and S. R. Hart (1995), Episodic trace element and isotopic variations in historical Mauna Loa lavas: Implications for magma and plume dynamics, in *Mauna Loa Revealed: Structure, Composition, History*

and Hazards, *Geophys. Monogr. Ser.*, vol. 92, edited by J. M. Rhodes and J. P. Lockwood, pp. 263–288, AGU, Washington, D. C.

Rhodes, J. M., and D. Weis (2001), Isotopic and Nb correlations in Hawaiian lavas: Evidence for a ubiquitous refractory plume component?, *Eos Trans. AGU*, *82*(48), Fall Meet. Suppl., F1314.

Rhodes, J. M., M. A. Dungan, D. P. Blanchard, and P. E. Long (1979), Magma mixing at mid-ocean ridges: Evidence from basalts drilled near 22°N on the mid-Atlantic ridge, *Tectonophysics*, *55*, 56–61.

Rhodes, J. M., K. P. Wenz, C. A. Neal, J. W. Sparks, and J. P. Lockwood (1989), Geochemical evidence for invasion of Kilauea's plumbing system by Mauna Loa magma, *Nature*, *337*, 257–260.

Ribe, N. M. (1988), Dynamical geochemistry of the Hawaiian plume, *Earth Planet. Sci. Lett,.*, *88*, 37–46.

Ribe, N. M., and U. R. Christenson (1999), The dynamic origin of Hawaiian volcanism, *Earth Planet. Sci. Lett.*, *171*, 517–531.

Roeder, P. L., and R. F. Emslie (1970), Olivine liquid equilibrium, *Contrib. Mineral. Petrol.*, *29*, 275–289.

Seaman, C. A., M. O. Garcia, and E. M. Stolper (Ed.) (2000), Hawaii Scientific Drilling Project-2, Core logs and summarizing data, rep., Calif. Inst. of Technol., Pasadena.

Sharp, W. D., B. D. Turrin, and M. A. Lanphere (1996), The $^{40}Ar/^{39}Ar$ and K/Ar dating of lavas from the Hilo 1-km core hole, Hawaii Scientific Drilling Project, *J. Geophys. Res.*, *101*, 11,607–11,616.

Spiegelman, M., and P. Kenyon (1992), The requirements for chemical disequilibrium during melt migration, *Earth Planet. Sci. Lett.*, *109*, 611–620.

Staudigal, H., A. Zindler, S. R. Hart, T. Leslie, C.-Y. Chen, and D. Clague (1984), The isotopic systematics of a juvenile intraplate volcano: Pb, Sr and Nd isotope ratios from Loihi seamount, Hawaii, *Earth Planet. Sci. Lett.*, *69*, 13–29.

Stearns, H. T. (1946), Geology of the Hawaiian Islands, *Hawaii Div. of Hydrogr. Bull.*, *8*, 105 pp.

Stracke, A., et al. (1999), Assessing the presence of garnet-pyroxenite in the mantle sources of basalts through combined hafnium-neodymium-thorium isotope systematics, *Geochem. Geophys. Geosyst.*, *1*, Paper number 1999GC000013.

Takahashi, E., and K. Nakajima (2002), Melting process in the Hawaiian plume: An experimental study, in *Hawaiian Volcanoes: Deep Underwater Perspectives*, *Geophys. Monogr. Ser.*, vol. 128, edited by E. Takahasi et al., pp. 403–418, AGU, Washington, D. C.

Takahashi, E., T. Shimazaki, Y. Tsuzaki, and H. Yoshida (1993), Melting study of a peridotite KLB-1 to 6.5 Gpa and the origin of basaltic magmas, 1993, 1998, *Philos. Trans. R. Soc. London Ser. A.*, *342*, 105–120.

Takahashi, E., K. Nakajima, and T. L. Wright (1998), Origin of Columbia River basalts: Melting model of an heterogeneous plume head, *Earth Planet. Sci. Lett.*, *162*, 63–80.

Tatsumoto, M. (1978), Isotopic composition of lead in oceanic basalt and its implication to mantle evolution, *Earth Planet. Sci. Lett.*, *38*, 13–29.

Watson, S., and D. Mackenzie (1991), Melt generation by plumes: A study of Hawaiian volcanism, *J. Petrol.*, *32*, 501–537.

West, H. B., D. C. Gerlach, W. P. Leeman, and M. O. Garcia (1987), Isotopic constraints on the origin of Hawaiian lavas from the Maui Volcanic Comples, Hawaii, *Nature*, *330*, 216–220.

Wilkinson, J. F. G., and H. D. Hensel (1988), The petrology of some picrites from Mauna Loa and Kilauea volcanoes, Hawaii, *Contrib. Mineral. Petrol.*, *98*, 326–345.

Wolfe, E. W., W. S. Wise, and B. G. Dalrymple (1997), The geology and petrology of Mauna Kea volcano, Hawaii: A study of postshield volcanism, *U.S. Geol. Soc. Prof.*, 1557.

Wright, T. L. (1971), Chemistry of Kilauea and Mauna Loa lavas in space and time, *U.S. Geol. Surv. Prof.*, *735*, 49 pp.

Wright, T. L. (1984), Origin of Hawaiian tholeiite: A metasomatic model, *J. Geophys. Res.*, *89*, 3233–3252.

Wright, T. L., and D. L. Peck (1978), Crystallization and differentiation of the Alae magma, Alae lava lake, Hawaii, *U.S. Geol. Surv. Prof.*, *935-C*, 20 pp.